Using the Jump Target to put Au^{79+} Ions into the AGS Dump

L. Ahrens, C. Gardner and P. Thieberger

October 28, 2009

Following are informal notes subject to change and correction. This is not a report.

1 Energy Deposition in the Jump Target

We have the following numbers:

1. The target is a tungsten foil 0.001 inches thick.
2. The density of tungsten is 19.3 g/cm^3.
3. This gives a surface density
$$\rho = 49 \text{ mg/cm}^2. \tag{1}$$
4. The kinetic energy of a gold ion at AGS extraction is 8.86 GeV per nucleon.
5. The rate of energy loss ($-dE/dx$) of a fully stripped gold ion traveling through tungsten at this energy is 8 MeV per mg/cm^2. This number comes from Peter Thieberger's plot of dE/dx versus E obtained using Ziegler's formulae.
6. The energy deposited by a gold ion traversing the foil at AGS extraction energy is then
$$\mathcal{E} = 8 \times 49 = 392 \text{ MeV}. \tag{2}$$
7. Using 1 eV $= 1.602176462(63) \times 10^{-19}$ we have
$$\mathcal{E} = 6.28 \times 10^{-11} \text{ joules}. \tag{3}$$
8. A single bunch at AGS extraction can have as many as $N = 1.5 \times 10^9$ ions per bunch. (The bunch length is $\tau = 16$ ns.)
9. A single bunch traversing the foil deposits energy
$$N\mathcal{E} = 0.0942 \text{ joules}. \tag{4}$$
10. Each AGS cycle four bunches pass through the foil. This gives a total energy deposition per AGS cycle of
$$4N\mathcal{E} = 0.377 \text{ joules}. \tag{5}$$

2 Temperature Rise

We have the following numbers:

1. The specific heat of tungsten is [10]

$$c = 0.132 \text{ J/(gK)}. \tag{6}$$

2. The melting point is 3414 C [10].

Let us assume that the area of foil exposed to beam is $w = 0.2$ mm wide and $h = 10$ mm high. The area is then

$$A = wh = 2 \times 10^{-2} \text{ cm}^2 \tag{7}$$

and the mass of tungsten exposed to beam is

$$\rho d A = 0.98 \text{ mg}. \tag{8}$$

The resulting rise in temperature, assuming no heat flow from the exposed part of the foil, is then

$$\Delta T = \frac{4N\mathcal{E}}{cd\rho A} = 2913 \text{ K}. \tag{9}$$

If the energy is deposited uniformly over time interval $\tau = 5$ ms, then the rate of temperature rise during this time (assuming no heat flow from the exposed part of the foil) is

$$\mathcal{K} = \frac{\Delta T}{\tau} = \frac{4N\mathcal{E}}{cd\rho A\tau} = 583 \text{ K/ms}. \tag{10}$$

3 Radiative Cooling during Energy Deposition

We have the following numbers:

1. The emissivity of tungsten at 3600 K is [9]

$$\epsilon = 0.35. \tag{11}$$

2. The Stefan-Boltzmann constant is

$$\sigma = 5.67 \times 10^{-8} \text{ W m}^{-2} \text{ K}^{-4}. \tag{12}$$

The rate at which energy is radiated from the foil is given by the Stefan-Boltzmann law [9]

$$P = A\epsilon\sigma \left(T^4 - T_W^4\right) \tag{13}$$

where T is the foil temperature and T_W is the temperature of the vacuum chamber wall.

Thus, as energy is deposited during collisions with gold ions, the rate of temperature change of the portion of foil exposed to beam is

$$\frac{dT}{dt} = \mathcal{K} - \frac{P}{c\rho A} = \mathcal{K} - \frac{\epsilon\sigma}{c\rho}\left(T^4 - T_W^4\right) \tag{14}$$

which we can write as

$$\frac{dT}{dt} = -\mathcal{C}\left(T^4 - \mathcal{A}^4\right) \tag{15}$$

where

$$\mathcal{C} = \frac{\epsilon\sigma}{c\rho}, \quad \mathcal{A}^4 = T_W^4 + \frac{\mathcal{K}}{\mathcal{C}}. \tag{16}$$

Integrating we obtain

$$\int_{T_1}^{T_2} \frac{dT}{T^4 - \mathcal{A}^4} = -\mathcal{C}\left(t_2 - t_1\right) \tag{17}$$

and using

$$\int \frac{dx}{a^4 - x^4} = \frac{1}{4a^3}\ln\left|\frac{a+x}{a-x}\right| + \frac{1}{2a^3}\arctan\left(\frac{x}{a}\right) \tag{18}$$

we have

$$\begin{aligned} 4\mathcal{A}^3\mathcal{C}\left(t_2 - t_1\right) &= \ln\left|\frac{\mathcal{A}+T_2}{\mathcal{A}-T_2}\right| + 2\arctan\left(\frac{T_2}{\mathcal{A}}\right) \\ &- \ln\left|\frac{\mathcal{A}+T_1}{\mathcal{A}-T_1}\right| - 2\arctan\left(\frac{T_1}{\mathcal{A}}\right). \end{aligned} \tag{19}$$

Thus

$$\exp\left\{4\mathcal{A}^3\mathcal{C}\left(t_2 - t_1\right)\right\} = \left|\frac{\mathcal{A}+T_2}{\mathcal{A}-T_2}\right|\left|\frac{\mathcal{A}-T_1}{\mathcal{A}+T_1}\right|\exp\left\{2(\theta_2 - \theta_1)\right\} \tag{20}$$

and

$$\left|\frac{\mathcal{A}+T_2}{\mathcal{A}-T_2}\right|\exp\left\{2\theta_2\right\} = \left|\frac{\mathcal{A}+T_1}{\mathcal{A}-T_1}\right|\exp\left\{2\theta_1 + 4\mathcal{A}^3\mathcal{C}\left(t_2 - t_1\right)\right\} \tag{21}$$

where

$$\theta_1 = \arctan\left(\frac{T_1}{\mathcal{A}}\right), \quad \theta_2 = \arctan\left(\frac{T_2}{\mathcal{A}}\right). \tag{22}$$

Given $\mathcal{A}$, T_1, $\mathcal{C}$ and $t_2 - t_1$ we can then obtain T_2.
We have

$$\mathcal{C} = 3.06840 \times 10^{-10} \tag{23}$$

and taking $\tau = 5$ ms gives

$$\mathcal{K} = 582.610 \text{ K/ms}. \tag{24}$$

Taking

$$T_W = 300, \quad t_2 - t_1 = \tau, \quad T_1 = 673.058 \tag{25}$$

then gives

$$\left|\frac{\mathcal{A} + T_2}{\mathcal{A} - T_2}\right| \exp\{2\theta_2\} = 8.78502 \tag{26}$$

and

$$T_2 = 3525.97 \text{ K}. \tag{27}$$

4 Radiative Cooling after Energy Deposition

After energy deposition we have $\mathcal{K} = 0$ and

$$\mathcal{A} = T_W. \tag{28}$$

Taking

$$T_W = 300, \quad T_1 = 3525.97, \quad t_2 - t_1 = 3.6 \text{ s} \tag{29}$$

then gives

$$\left|\frac{T_W + T_2}{T_W - T_2}\right| \exp\{2\theta_2\} = 26.0942 \tag{30}$$

and

$$T_2 = 673.058 \text{ K}. \tag{31}$$

5 Cooling by Heat Conduction

We have the following numbers:

1. The specific heat of tungsten is $c = 0.132$ J/(gK) [10].
2. The density is $\rho = 19.3$ g/cm^3 [10].
3. The thermal conductivity at 300 K is $K = 174$ W/(mK).
4. The thermal conductivity at 1800 K is $K = 101$ W/(mK).
5. The melting point is 3414 C [10].

The energy deposited is $4N\mathcal{E} = 0.377$ joules.

The time interval is $\tau = 5$ ms.

The instantaneous power is $P = 4N\mathcal{E}/\tau = 75.4$ watts.

The foil thickness is $d = 0.0254$ mm.

The beam width on the foil is $w = 0.2$ mm.

The beam height on the foil is $h = 10$ mm.

The heat flow area is $a = dh = 0.254 \times 10^{-6}$ m^2.

We have [11, 12, 13, 14, 15]

$$\nabla \cdot \mathbf{h} + \frac{dq}{dt} = S \tag{32}$$

where

$$\mathbf{h} = -K\nabla T \tag{33}$$

and

$$\frac{dq}{dt} = c\rho \frac{\partial T}{\partial t}. \tag{34}$$

The source term

$$S = \frac{P}{dA} = \frac{4N\mathcal{E}}{dA\tau} = 1484 \text{ W/mm}^3 \tag{35}$$

is due to energy deposition in the foil; it is nonzero only where the foil is exposed to beam.

For the case

$$\nabla K = \mathbf{0} \tag{36}$$

we then have

$$\nabla^2 T - \frac{c\rho}{K}\frac{\partial T}{\partial t} = -\frac{S}{K} \tag{37}$$

where c is the specific heat, ρ is the density and K is the thermal conductivity.

For the case in which the temperature depends only on x and t we have

$$\frac{\partial^2 T}{\partial x^2} - \frac{c\rho}{K}\frac{\partial T}{\partial t} = -\frac{S}{K}. \tag{38}$$

Note that if

$$\widehat{T} = T - T_I \tag{39}$$

where T_I is a constant, then

$$\frac{\partial^2 \widehat{T}}{\partial x^2} - \frac{c\rho}{K}\frac{\partial \widehat{T}}{\partial t} = -\frac{S}{K}. \tag{40}$$

Thus if we have a non-homogeneous boundry condition $T = T_I$, this can be changed to a homogeneous one by working with $\widehat{T}$.

6 Steady State

For the steady state we have

$$\frac{\partial T}{\partial t} = 0 \tag{41}$$

and

$$\frac{\partial^2 T}{\partial x^2} = -\frac{S}{K} \tag{42}$$

where

$$\frac{S}{K} = \frac{P}{dAK} \tag{43}$$

and

$$A = wh. \tag{44}$$

Thus we have

$$T(x) = T_0 - gx - \frac{S}{2K}x^2, \quad 0 \le x < w \tag{45}$$

$$T(x) = T_w - G(x - w), \quad w \le x \le D \tag{46}$$

and

$$\frac{\partial T}{\partial x} = -g - \frac{S}{K}x, \quad 0 \le x < w \tag{47}$$

$$\frac{\partial T}{\partial x} = -G, \quad w \le x \le D. \tag{48}$$

We want $T(x)$ and $\partial T/\partial x$ to be continuous at $x = w$. This gives

$$T_w = T_0 - gw - \frac{S}{2K}\, w^2 \tag{49}$$

and

$$G = g + \frac{Sw}{K}. \tag{50}$$

We also have the boundry condition

$$\left(\frac{\partial T}{\partial x}\right)_{x=0} = 0 \tag{51}$$

which gives

$$g = 0. \tag{52}$$

Thus

$$G = \frac{Sw}{K} = \frac{Pw}{dAK} = \frac{P}{aK} \tag{53}$$

and

$$\left(\frac{\partial T}{\partial x}\right)_{x=w} = -\frac{P}{aK} \tag{54}$$

where we have used

$$A = wh, \quad a = dh. \tag{55}$$

Thus

$$T(x) = T_0 - \frac{S}{2K}\, x^2, \quad 0 \le x < w \tag{56}$$

and

$$T(x) = T_w - \frac{Sw}{K}(x - w), \quad w \le x \le D \tag{57}$$

where

$$T_w = T_0 - \frac{S}{2K}\, w^2. \tag{58}$$

We also have

$$T_D = T(D) = T_w - G(D - w) \tag{59}$$

$$T_w = T_D + G(D - w) \tag{60}$$

$$T_0 = T_w + \frac{Sw^2}{2K} \tag{61}$$

$$T_0 = T_D + GD - \frac{Sw^2}{2K} \tag{62}$$

$$T_0 = T_D + \frac{PD}{aK} - \frac{Pw}{2aK} \tag{63}$$

$$T_0 - T_D = \frac{P}{aK}\left\{D - \frac{w}{2}\right\} \tag{64}$$

$$T_w - T_D = \frac{P}{aK}(D - w) \tag{65}$$

and

$$T_0 - T_w = \frac{P}{aK}\,\frac{w}{2}. \tag{66}$$

Taking $K = 100$ W/(mK) we have

$$G = \frac{P}{aK} = 2969 \text{ K/mm}. \tag{67}$$

7 Semi-Infinite Solid with Constant Surface Heat Rate

Here we follow the treatment of Eckert and Drake [16].

Suppose

$$\frac{\partial^2 T}{\partial x^2} - \frac{c\rho}{K}\,\frac{\partial T}{\partial t} = 0 \tag{68}$$

and let

$$q = -K\frac{\partial T}{\partial x}. \tag{69}$$

Then

$$\frac{\partial q}{\partial x} = -K\frac{\partial^2 T}{\partial x^2} = -c\rho\,\frac{\partial T}{\partial t} \tag{70}$$

$$\frac{\partial^2 q}{\partial x^2} = -c\rho\,\frac{\partial^2 T}{\partial x \partial t} = \frac{c\rho}{K}\,\frac{\partial q}{\partial t} \tag{71}$$

$$\frac{\partial q}{\partial t} = \alpha\,\frac{\partial^2 q}{\partial x^2} \tag{72}$$

where

$$\alpha = \frac{K}{c\rho}. \tag{73}$$

We have

$$\operatorname{erf} y = \frac{2}{\sqrt{\pi}} \int_0^y \exp(-s^2)\, ds \tag{74}$$

$$\frac{d}{dy} \operatorname{erf} y = \frac{2}{\sqrt{\pi}} \exp(-y^2) \tag{75}$$

$$\frac{d^2}{dy^2} \operatorname{erf} y = -2y \operatorname{erf} y \tag{76}$$

$$\operatorname{erfc} y = 1 - \operatorname{erf} y \tag{77}$$

$$\operatorname{ierfc} y = \int_y^\infty \operatorname{erfc} t\, dt \tag{78}$$

and

$$\operatorname{ierfc} y = \frac{1}{\sqrt{\pi}} \exp(-y^2) - y \operatorname{erfc} y. \tag{79}$$

Consider

$$q(x,t) = q_0 \left\{ 1 - \operatorname{erf} \frac{x}{\sqrt{4\alpha t}} \right\} \tag{80}$$

$$\frac{\partial q}{\partial x} = -\frac{2q_0}{\sqrt{4\pi\alpha t}} \exp\left(-\frac{x^2}{4\alpha t}\right) \tag{81}$$

$$\frac{\partial^2 q}{\partial x^2} = \frac{2q_0}{\sqrt{4\pi\alpha t}} \frac{2x}{4\alpha t} \exp\left(-\frac{x^2}{4\alpha t}\right) \tag{82}$$

$$\alpha \frac{\partial^2 q}{\partial x^2} = \frac{q_0 x}{t\sqrt{4\pi\alpha t}} \exp\left(-\frac{x^2}{4\alpha t}\right) \tag{83}$$

$$\frac{\partial q}{\partial t} = -\frac{q_0 x}{\sqrt{4\alpha}} \left\{ -\frac{1}{2} t^{-3/2} \right\} \frac{2}{\sqrt{\pi}} \exp\left(-\frac{x^2}{4\alpha t}\right). \tag{84}$$

Thus we have

$$\frac{\partial q}{\partial t} = \frac{q_0 x}{t\sqrt{4\pi\alpha t}} \exp\left(-\frac{x^2}{4\alpha t}\right) = \alpha \frac{\partial^2 q}{\partial x^2} \tag{85}$$

$$q(0,t) = q_0, \quad q(x,0) = 0 \tag{86}$$

$$-K\left\{T(\infty,t) - T(x,t)\right\} = \int_x^\infty q(s,t)\,ds \tag{87}$$

$$T(x,t) - T(\infty,t) = \frac{q_0}{K}\int_x^\infty \operatorname{erfc}\left(\frac{s}{\sqrt{4\alpha t}}\right)\,ds \tag{88}$$

$$u = \frac{s}{\sqrt{4\alpha t}}, \quad ds = du\sqrt{4\alpha t} \tag{89}$$

$$\Delta T = T(x,t) - T(\infty,t) \tag{90}$$

$$\Delta T = \frac{q_0}{K}\sqrt{4\alpha t}\int_v^\infty \operatorname{erfc} u\,du \tag{91}$$

$$v = \frac{x}{\sqrt{4\alpha t}} \tag{92}$$

$$\Delta T = \frac{q_0}{K}\sqrt{4\alpha t}\,\operatorname{ierfc}\left(\frac{x}{\sqrt{4\alpha t}}\right) \tag{93}$$

$$\operatorname{ierfc} y = \frac{1}{\sqrt{\pi}}\exp(-y^2) - y\operatorname{erfc} y \tag{94}$$

$$\Delta T(x,t) = \frac{q_0}{K}\sqrt{4\alpha t}\left\{\frac{1}{\sqrt{\pi}}\exp\left(-\frac{x^2}{4\alpha t}\right) - \frac{x}{\sqrt{4\alpha t}}\operatorname{erfc}\left(\frac{x}{\sqrt{4\alpha t}}\right)\right\} \tag{95}$$

$$\Delta T(x,t) = T_0(t)F(x,t) \tag{96}$$

$$\Delta T_0(t) = \frac{q_0}{K}\sqrt{\frac{4\alpha t}{\pi}} \tag{97}$$

$$F(x,t) = \exp\left(-\frac{x^2}{4\alpha t}\right) - \sqrt{\frac{\pi x^2}{4\alpha t}}\operatorname{erfc}\left(\frac{x}{\sqrt{4\alpha t}}\right). \tag{98}$$

Here

$$q_0 = KG, \quad G = \frac{E}{a\tau K}, \quad \alpha = \frac{K}{c\rho} \tag{99}$$

which gives

$$\Delta T_0(t) = \frac{E}{a\tau K}\sqrt{\frac{4Kt}{\pi c\rho}} = \frac{2E}{a\tau}\sqrt{\frac{t}{\pi c\rho K}} \tag{100}$$

and

$$\Delta T_0(\tau) = \frac{2E}{a\sqrt{\tau}}\sqrt{\frac{1}{\pi c\rho K}}. \tag{101}$$

Taking

1. $c = 0.132$ J/(gK)
2. $\rho = 19.3$ g/cm^3
3. $K = 1.0$ W/(cm K)

we have

$$\sqrt{\frac{1}{\pi c\rho K}} = \sqrt{\frac{1}{8.0035}}\left(\frac{\mathrm{K\,cm^2}\sqrt{\mathrm{s}}}{\mathrm{J}}\right) \tag{102}$$

and taking

1. $E = 0.377$ J
2. $a = 0.00254$ cm^2
3. $\tau = 0.005$ s

gives

$$\Delta T_0(\tau) = 1484\ \mathrm{K}. \tag{103}$$

We also have

$$F(x,\tau) = \exp\left(-\frac{x^2}{4\alpha\tau}\right) - \sqrt{\frac{\pi x^2}{4\alpha\tau}}\,\mathrm{erfc}\left(\frac{x}{\sqrt{4\alpha\tau}}\right) \tag{104}$$

where

$$4\alpha\tau = \frac{4K\tau}{c\rho} = 0.00785\ \mathrm{cm}^2 \tag{105}$$

and

$$\sqrt{4\alpha\tau} = 0.0886\ \mathrm{cm}. \tag{106}$$

8 Stay-Clear Region at AGS Injection

Horizontal limiting aperture in AGS is A5 kicker which has half aperture of 2.532 inches. Taking $\beta_x = 23$ m at A5 gives horizontal acceptance $\pi e_x = 180\pi$ mm mrad.

Vertical limiting aperture is in the section 11 main magnets. Here the vertical half-aperture is 1.531 inches. Taking $\beta_y = 23$ here gives vertical acceptance $\pi e_y = 66\pi$ mm mrad.

Thus if we do not want to intercept any beam with the jump target, we must stay clear of the region defined by

$$-\sqrt{e_x\beta_x} \leq X \leq \sqrt{e_x\beta_x} \tag{107}$$

and

$$-\sqrt{e_y\beta_y} \leq Y \leq \sqrt{e_y\beta_y} \tag{108}$$

where

$$\beta_x = 11 \text{ m}, \quad \beta_y = 21 \text{ m}. \tag{109}$$

Using the values of e_x and e_y given above we then have

$$|X| \leq 44 \text{ mm}, \quad |Y| \leq 37 \text{ mm}. \tag{110}$$

9 Transport of Stripped and Unstripped Beam

We have

$$\mathbf{X} = \mathbf{M}\mathbf{X}_0 + \frac{\Delta p}{p}\left(\mathbf{D} - \mathbf{M}\mathbf{D}_0\right) + \left(1 - \frac{\Delta p}{p}\right)\left(\mathbf{d} - \mathbf{M}\mathbf{d}_0\right) \tag{111}$$

where

$$\mathbf{X} = \begin{pmatrix} X \\ X' \end{pmatrix}, \quad \mathbf{X}_0 = \begin{pmatrix} X_0 \\ X'_0 \end{pmatrix} \tag{112}$$

$$\mathbf{D} = \begin{pmatrix} D \\ D' \end{pmatrix}, \quad \mathbf{D}_0 = \begin{pmatrix} D_0 \\ D'_0 \end{pmatrix} \tag{113}$$

$$\mathbf{d} = \begin{pmatrix} d \\ d' \end{pmatrix}, \quad \mathbf{d}_0 = \begin{pmatrix} d_0 \\ d'_0 \end{pmatrix}. \tag{114}$$

Thus

$$
\begin{aligned}
X &= M_{11}X_0 + M_{12}X_0' \\
&+ \frac{\Delta p}{p}\left(D - M_{11}D_0 - M_{12}D_0'\right) \\
&+ \left(1 - \frac{\Delta p}{p}\right)\left(d - M_{11}d_0 - M_{12}d_0'\right) \qquad (115)
\end{aligned}
$$

and

$$
\begin{aligned}
X' &= M_{21}X_0 + M_{22}X_0' \\
&+ \frac{\Delta p}{p}\left(D' - M_{21}D_0 - M_{22}D_0'\right) \\
&+ \left(1 - \frac{\Delta p}{p}\right)\left(d' - M_{21}d_0 - M_{22}d_0'\right) \qquad (116)
\end{aligned}
$$

where

$$M_{11} = \sqrt{\beta/\beta_0}\,(C + \alpha_0 S), \quad M_{12} = \sqrt{\beta\beta_0}\,S \qquad (117)$$

$$M_{21} = -\left(\frac{\alpha - \alpha_0}{\sqrt{\beta\beta_0}}\right)C - \left(\frac{1 + \alpha\alpha_0}{\sqrt{\beta\beta_0}}\right)S, \quad M_{22} = \sqrt{\beta_0/\beta}\,(C - \alpha S). \qquad (118)$$

Let

$$\mathcal{X}_0 = M_{11}X_0 + M_{12}X_0' \qquad (119)$$

$$\Delta D = D - M_{11}D_0 - M_{12}D_0' \qquad (120)$$

$$\Delta d = d - M_{11}d_0 - M_{12}d_0' \qquad (121)$$

$$\mathcal{X} = \mathcal{X}_0 + \Delta d \qquad (122)$$

and

$$\mathcal{X}_0' = M_{21}X_0 + M_{22}X_0' \qquad (123)$$

$$\Delta D' = D' - M_{21}D_0 - M_{22}D_0' \qquad (124)$$

$$\Delta d' = d' - M_{21}d_0 - M_{22}d_0' \qquad (125)$$

$$\mathcal{X}' = \mathcal{X}_0' + \Delta d'. \qquad (126)$$

Then

$$X = \mathcal{X} + \frac{\Delta p}{p}\left(\Delta D - \Delta d\right) \qquad (127)$$

$$X' = \mathcal{X}' + \frac{\Delta p}{p}\left(\Delta D' - \Delta d'\right). \qquad (128)$$

Here $\mathcal{X}$ is the Au^{77+} trajectory and X is the Au^{79+} trajectory. $\mathcal{X}_0$ is the trajectory of Au^{77+} with no perturbing dipoles between the launch point and the observation point.

For any Y_0 and Y_0' we have

$$M_{11}Y_0 + M_{12}Y_0' = \sqrt{\beta/\beta_0}\left\{CY_0 + S\left(\alpha_0 Y_0 + \beta_0 Y_0'\right)\right\} \tag{129}$$

$$M_{21}Y_0 + M_{22}Y_0' = \frac{1}{\sqrt{\beta\beta_0}}\left\{(C-\alpha S)\left(\alpha_0 Y_0 + \beta_0 Y_0'\right) - (S+\alpha C)Y_0\right\}. \tag{130}$$

Thus we have

$$\mathcal{X}_0 = \sqrt{\beta/\beta_0}\left\{CX_0 + S\left(\alpha_0 X_0 + \beta_0 X_0'\right)\right\} \tag{131}$$

$$\Delta D = D - \sqrt{\beta/\beta_0}\left\{CD_0 + S\left(\alpha_0 D_0 + \beta_0 D_0'\right)\right\} \tag{132}$$

$$\Delta d = d - \sqrt{\beta/\beta_0}\left\{Cd_0 + S\left(\alpha_0 d_0 + \beta_0 d_0'\right)\right\} \tag{133}$$

and

$$\mathcal{X}_0' = \frac{1}{\sqrt{\beta\beta_0}}\left\{(C-\alpha S)\left(\alpha_0 X_0 + \beta_0 X_0'\right) - (S+\alpha C)X_0\right\} \tag{134}$$

$$\Delta D' = D' - \frac{1}{\sqrt{\beta\beta_0}}\left\{(C-\alpha S)\left(\alpha_0 D_0 + \beta_0 D_0'\right) - (S+\alpha C)D_0\right\} \tag{135}$$

$$\Delta d' = d' - \frac{1}{\sqrt{\beta\beta_0}}\left\{(C-\alpha S)\left(\alpha_0 d_0 + \beta_0 d_0'\right) - (S+\alpha C)d_0\right\}. \tag{136}$$

Now, since the stripper always strips the maximum amplitude ions, we have

$$\alpha_0\left(X_0 - d_0\right) + \beta_0\left(X_0' - d_0'\right) = 0 \tag{137}$$

which gives

$$\alpha_0 X_0 + \beta_0 X_0' = \alpha_0 d_0 + \beta_0 d_0' \tag{138}$$

$$\mathcal{X}_0 = \sqrt{\beta/\beta_0}\left\{CX_0 + S\left(\alpha_0 d_0 + \beta_0 d_0'\right)\right\} \tag{139}$$

$$\mathcal{X}_0' = \frac{1}{\sqrt{\beta\beta_0}}\left\{(C-\alpha S)\left(\alpha_0 d_0 + \beta_0 d_0'\right) - (S+\alpha C)X_0\right\} \tag{140}$$

$$\mathcal{X} = d + \sqrt{\beta/\beta_0}\,C\left(X_0 - d_0\right) \tag{141}$$

and

$$\mathcal{X}' = d' - \frac{1}{\sqrt{\beta\beta_0}}(S + \alpha C)(X_0 - d_0). \tag{142}$$

Let

$$X_0 = d_0 - \sqrt{\epsilon\beta_0} \tag{143}$$

$$X_d = d - \sqrt{\epsilon\beta}. \tag{144}$$

The separation between the Au^{79+} trajectory and the circulating Au^{77+} beam envelope is then

$$X - X_d = \mathcal{X} - X_d + \frac{\Delta p}{p}\,(\Delta D - \Delta d) \tag{145}$$

where

$$\mathcal{X} = d + \sqrt{\beta/\beta_0}\,C\,(X_0 - d_0) = d - C\sqrt{\epsilon\beta} \tag{146}$$

$$\mathcal{X} - X_d = (1 - C)\sqrt{\epsilon\beta}. \tag{147}$$

Thus the separation is

$$X - X_d = (1 - C)\sqrt{\epsilon\beta} + \frac{\Delta p}{p}\,(\Delta D - \Delta d) \tag{148}$$

where

$$\Delta D = D - \sqrt{\beta/\beta_0}\,\{CD_0 + S\,(\alpha_0 D_0 + \beta_0 D_0')\} \tag{149}$$

$$\Delta d = d - \sqrt{\beta/\beta_0}\,\{Cd_0 + S\,(\alpha_0 d_0 + \beta_0 d_0')\}\,. \tag{150}$$

Writing

$$X = M_{11}X_0 + M_{12}X_0' + \Delta d + \frac{\Delta p}{p}\,(\Delta D - \Delta d) \tag{151}$$

we see that if X_0, X_0', and Δd are held fixed while d_0 and d_0' are varied, then X will remain unchanged. This means that Au^{79+} ions born at s_0 under these conditions will all end up at the same X. Here

$$\Delta d = d - M_{11}d_0 - M_{12}d_0' \tag{152}$$

$$\Delta D = D - M_{11}D_0 - M_{12}D_0' \tag{153}$$

and

$$\alpha_0 X_0 + \beta_0 X_0' = \alpha_0 d_0 + \beta_0 d_0'. \tag{154}$$

Thus d_0 and d_0' must be varied in a way that keeps $\alpha_0 d_0 + \beta_0 d_0'$ constant.

Consider now the case in which

$$\alpha_0 = 0, \quad \alpha = 0, \quad \beta = \beta_0 \tag{155}$$

$$d_0 = 0, \quad d'_0 = 0, \quad d = 0, \quad d' = 0 \tag{156}$$

$$D'_0 = 0, \quad D' = 0, \quad D = D_0. \tag{157}$$

We then have

$$X = CX_0 + \frac{\Delta p}{p}\,(1 - C)\,D \tag{158}$$

where

$$\frac{\Delta p}{p} = -\frac{2}{77} = -0.02597. \tag{159}$$

For a tune of 8.75 the average betatron phase advance per cell in the AGS is 52.5°. This gives

$$C = 0.60876 \tag{160}$$

and

$$X = (0.60876)X_0 - (0.01016)D. \tag{161}$$

The average phase advance for two cells would be 105° which gives

$$C = -0.25882 \tag{162}$$

and

$$X = (-0.25882)X_0 - (0.03270)D. \tag{163}$$

10 Four-dimensional Ellipsoid

$$\mathbf{Z}^{\dagger}\mathbf{E}^{-1}\mathbf{Z} = \epsilon \tag{164}$$

$$\mathbf{Z}^{\dagger}(\epsilon\mathbf{E})^{-1}\mathbf{Z} = 1 \tag{165}$$

$$\mathbf{Z} = \begin{pmatrix} \mathbf{X} \\ \mathbf{Y} \end{pmatrix}, \quad \mathbf{X} = \begin{pmatrix} X \\ X' \end{pmatrix}, \quad \mathbf{Y} = \begin{pmatrix} Y \\ Y' \end{pmatrix} \tag{166}$$

$$\epsilon\mathbf{E} = \begin{pmatrix} \epsilon_x\mathbf{A} & \mathbf{0} \\ \mathbf{0} & \epsilon_y\mathbf{B} \end{pmatrix} \tag{167}$$

$$(\epsilon\mathbf{E})^{-1} = \begin{pmatrix} (\epsilon_x\mathbf{A})^{-1} & \mathbf{0} \\ \mathbf{0} & (\epsilon_y\mathbf{B})^{-1} \end{pmatrix} \tag{168}$$

$$\left\{\mathbf{X}^\dagger(\epsilon_x\mathbf{A})^{-1}\mathbf{X}\right\}+\left\{\mathbf{Y}^\dagger(\epsilon_y\mathbf{B})^{-1}\mathbf{Y}\right\}=1 \tag{169}$$

$$\mathbf{A}=\mathcal{F}\mathcal{F}^\dagger,\quad \mathbf{B}=\mathcal{G}\mathcal{G}^\dagger \tag{170}$$

$$\mathcal{F}=\frac{1}{\sqrt{\beta_x}}\left(\begin{array}{rr}\beta_x & 0\\ -\alpha_x & 1\end{array}\right),\quad \mathcal{G}=\frac{1}{\sqrt{\beta_y}}\left(\begin{array}{rr}\beta_y & 0\\ -\alpha_y & 1\end{array}\right) \tag{171}$$

$$\widehat{\mathbf{X}}=(\sqrt{\epsilon_x}\,\mathcal{F})^{-1}\mathbf{X},\quad \widehat{\mathbf{Y}}=(\sqrt{\epsilon_y}\,\mathcal{G})^{-1}\mathbf{Y} \tag{172}$$

$$\widehat{\mathbf{X}}^\dagger\widehat{\mathbf{X}}=\mathbf{X}^\dagger(\epsilon_x\mathbf{A})^{-1}\mathbf{X} \tag{173}$$

$$\widehat{\mathbf{Y}}^\dagger\widehat{\mathbf{Y}}=\mathbf{Y}^\dagger(\epsilon_y\mathbf{B})^{-1}\mathbf{Y} \tag{174}$$

$$\widehat{\mathbf{X}}^\dagger\widehat{\mathbf{X}}+\widehat{\mathbf{Y}}^\dagger\widehat{\mathbf{Y}}=1 \tag{175}$$

$$\widehat{\mathbf{X}}=\left(\begin{array}{c}\widehat{X}\\ \widehat{X}'\end{array}\right),\quad \widehat{\mathbf{Y}}=\left(\begin{array}{c}\widehat{Y}\\ \widehat{Y}'\end{array}\right) \tag{176}$$

$$\widehat{X}^2+\widehat{X}'^2+\widehat{Y}^2+\widehat{Y}'^2=1 \tag{177}$$

$$\widehat{X}=\left(\sqrt{\epsilon_x\beta_x}\right)^{-1}X,\quad \widehat{Y}=\left(\sqrt{\epsilon_y\beta_y}\right)^{-1}Y \tag{178}$$

$$\widehat{Y}=\widehat{M}\widehat{X}+\widehat{B} \tag{179}$$

$$Y=MX+B \tag{180}$$

$$M=\widehat{M}\sqrt{\frac{\epsilon_y\beta_y}{\epsilon_x\beta_x}},\quad B=\widehat{B}\sqrt{\epsilon_y\beta_y} \tag{181}$$

Note that for round beams we have

$$\epsilon_y\beta_y=\epsilon_x\beta_x \tag{182}$$

and

$$\widehat{M}=M. \tag{183}$$

11 Appendix

$$\mathbf{T}_i = \begin{pmatrix} a_i & b_i & e_i \\ f_i & g_i & e'_i \\ 0 & 0 & 1 \end{pmatrix} = \begin{pmatrix} \mathbf{M}_i & \mathbf{e}_i \\ 0 & 1 \end{pmatrix} \tag{184}$$

$$\mathbf{M}_i = \begin{pmatrix} a_i & b_i \\ f_i & g_i \end{pmatrix}, \quad \mathbf{e}_i = \begin{pmatrix} e_i \\ e'_i \end{pmatrix} \tag{185}$$

$$\mathbf{Z} = \begin{pmatrix} X \\ X' \\ \Delta p/p \end{pmatrix} = \begin{pmatrix} \mathbf{X} \\ \Delta p/p \end{pmatrix} \tag{186}$$

$$\mathbf{Z}_0 = \begin{pmatrix} X_0 \\ X'_0 \\ \Delta p/p \end{pmatrix} = \begin{pmatrix} \mathbf{X}_0 \\ \Delta p/p \end{pmatrix} \tag{187}$$

$$\Theta_i = K \begin{pmatrix} 0 \\ \phi_i \\ 0 \end{pmatrix} = K \begin{pmatrix} \Phi_i \\ 0 \end{pmatrix} \tag{188}$$

$$\mathbf{X} = \begin{pmatrix} X \\ X' \end{pmatrix}, \quad \mathbf{X}_0 = \begin{pmatrix} X_0 \\ X'_0 \end{pmatrix}, \quad \Phi_i = \begin{pmatrix} \phi_i \\ 0 \end{pmatrix} \tag{189}$$

$$\begin{aligned} \mathbf{Z} &= \mathbf{T}_N \mathbf{T}_{N-1} \cdots \mathbf{T}_1 \mathbf{Z}_0 \\ &+ \mathbf{T}_N \mathbf{T}_{N-1} \cdots \mathbf{T}_2 \Theta_1 \\ &+ \mathbf{T}_N \mathbf{T}_{N-1} \cdots \mathbf{T}_3 \Theta_2 \\ &+ \mathbf{T}_N \mathbf{T}_{N-1} \cdots \mathbf{T}_4 \Theta_3 \\ &\vdots \\ &+ \mathbf{T}_N \Theta_{N-1} \end{aligned} \tag{190}$$

$$\mathbf{T}_2 \mathbf{T}_1 = \begin{pmatrix} \mathbf{M}_2 & \mathbf{e}_2 \\ 0 & 1 \end{pmatrix} \begin{pmatrix} \mathbf{M}_1 & \mathbf{e}_1 \\ 0 & 1 \end{pmatrix} \tag{191}$$

$$\mathbf{T}_2 \mathbf{T}_1 = \begin{pmatrix} \mathbf{M}_2 \mathbf{M}_1 & \mathbf{M}_2 \mathbf{e}_1 + \mathbf{e}_2 \\ 0 & 1 \end{pmatrix} \tag{192}$$

$$\mathbf{T}_3\mathbf{T}_2\mathbf{T}_1 = \begin{pmatrix} \mathbf{M}_3 & \mathbf{e}_3 \\ 0 & 1 \end{pmatrix} \begin{pmatrix} \mathbf{M}_2\mathbf{M}_1 & \mathbf{M}_2\mathbf{e}_1 + \mathbf{e}_2 \\ 0 & 1 \end{pmatrix} \tag{193}$$

$$\mathbf{T}_3\mathbf{T}_2\mathbf{T}_1 = \begin{pmatrix} \mathbf{M}_3\mathbf{M}_2\mathbf{M}_1 & \mathbf{M}_3\mathbf{M}_2\mathbf{e}_1 + \mathbf{M}_3\mathbf{e}_2 + \mathbf{e}_3 \\ 0 & 1 \end{pmatrix} \tag{194}$$

$$\begin{aligned} \mathbf{X} &= \mathbf{M}_N\mathbf{M}_{N-1}\cdots\mathbf{M}_1\mathbf{X}_0 \\ &+ \mathbf{M}_N\mathbf{M}_{N-1}\cdots\mathbf{M}_2\left(\frac{\Delta p}{p}\,\mathbf{e}_1 + K\Phi_1\right) \\ &+ \mathbf{M}_N\mathbf{M}_{N-1}\cdots\mathbf{M}_3\left(\frac{\Delta p}{p}\,\mathbf{e}_2 + K\Phi_2\right) \\ &+ \mathbf{M}_N\mathbf{M}_{N-1}\cdots\mathbf{M}_4\left(\frac{\Delta p}{p}\,\mathbf{e}_3 + K\Phi_3\right) \\ &\vdots \\ &+ \mathbf{M}_N\left(\frac{\Delta p}{p}\,\mathbf{e}_{N-1} + K\Phi_{N-1}\right) + \frac{\Delta p}{p}\,\mathbf{e}_N \end{aligned} \tag{195}$$

$$\begin{aligned} \mathbf{d} &= \mathbf{M}_N\mathbf{M}_{N-1}\cdots\mathbf{M}_1\mathbf{d}_0 \\ &+ \mathbf{M}_N\mathbf{M}_{N-1}\cdots\mathbf{M}_2\Phi_1 \\ &+ \mathbf{M}_N\mathbf{M}_{N-1}\cdots\mathbf{M}_3\Phi_2 \\ &+ \mathbf{M}_N\mathbf{M}_{N-1}\cdots\mathbf{M}_4\Phi_3 \\ &\vdots \\ &+ \mathbf{M}_N\Phi_{N-1} \end{aligned} \tag{196}$$

$$\begin{aligned} \mathbf{D} &= \mathbf{M}_N\mathbf{M}_{N-1}\cdots\mathbf{M}_1\mathbf{D}_0 \\ &+ \mathbf{M}_N\mathbf{M}_{N-1}\cdots\mathbf{M}_2\mathbf{e}_1 \\ &+ \mathbf{M}_N\mathbf{M}_{N-1}\cdots\mathbf{M}_3\mathbf{e}_2 \\ &+ \mathbf{M}_N\mathbf{M}_{N-1}\cdots\mathbf{M}_4\mathbf{e}_3 \\ &\vdots \\ &+ \mathbf{M}_N\mathbf{e}_{N-1} + \mathbf{e}_N \end{aligned} \tag{197}$$

$$
\begin{aligned}
\mathbf{X} &= \mathbf{M}_N\mathbf{M}_{N-1}\cdots\mathbf{M}_1\mathbf{X}_0 \\
&+ \mathbf{M}_N\mathbf{M}_{N-1}\cdots\mathbf{M}_2\left(\frac{\Delta p}{p}\,\mathbf{e}_1 + K\Phi_1\right) \\
&+ \mathbf{M}_N\mathbf{M}_{N-1}\cdots\mathbf{M}_3\left(\frac{\Delta p}{p}\,\mathbf{e}_2 + K\Phi_2\right) \\
&+ \mathbf{M}_N\mathbf{M}_{N-1}\cdots\mathbf{M}_4\left(\frac{\Delta p}{p}\,\mathbf{e}_3 + K\Phi_3\right) \\
&\vdots \\
&+ \mathbf{M}_N\left(\frac{\Delta p}{p}\,\mathbf{e}_{N-1} + K\Phi_{N-1}\right) + \frac{\Delta p}{p}\,\mathbf{e}_N \qquad (198)
\end{aligned}
$$

where

$$K = 1 - \frac{\Delta p}{p}. \tag{199}$$

Thus

$$\mathbf{X} = \mathbf{M}\mathbf{X}_0 + \frac{\Delta p}{p}\left(\mathbf{D} - \mathbf{M}\mathbf{D}_0\right) + \left(1 - \frac{\Delta p}{p}\right)\left(\mathbf{d} - \mathbf{M}\mathbf{d}_0\right) \tag{200}$$

where

$$\mathbf{M} = \mathbf{M}_N\mathbf{M}_{N-1}\cdots\mathbf{M}_1. \tag{201}$$

This also can be written as

$$\mathbf{X} - \frac{\Delta p}{p}\,\mathbf{D} - K\mathbf{d} = \mathbf{M}\left\{\mathbf{X}_0 - \frac{\Delta p}{p}\,\mathbf{D}_0 - K\mathbf{d}_0\right\}. \tag{202}$$

References

[1] C.J. Gardner, "Modeling Backleg Winding Bumps with the BEAM Program", AGS/AD/Tech. Note No. 341, August 21, 1990.

[2] C.J. Gardner, "The New Booster Dump and Dump Bumps", C-A/AP/Note 46, March 2001.

[3] C.J. Gardner, "Multi-turn Injection of Heavy Ions in Booster with the H-Minus Injection Foil Inserted", C-A/AP/Note 64, September 2001.

[4] C-A Department Drawing D08-M-227-5, July 1997.

[5] P. Carolan, et al, "Another Look at Apertures in the AGS", AGS/AD/Tech Note 355, November 15, 1991.

[6] L.A. Ahrens and C.J. Gardner, "Determination of the AGS Injection Kicker Strength from Beam Measurements", C-A/AP/Note 91, December 2002.

[7] C.J. Gardner, "Notes on Orbit Equations in the AGS", C-A/AP/Note 164, September 2004.

[8] C.J. Gardner, "Ags Injection with an Additional Kicker in the A10 Straight Section", C-A/AP/Note 217, September 2005.

[9] M.W. Zemansky, Heat and Thermodynamics, 5th Edition, McGraw-Hill, pp. 99–103 (1968)

[10] Periodic Table Online, CRC Press.

[11] R.P. Feynman, R.B. Leighton and M. Sands, The Feynman Lectures on Physics, Volume II, Addison-Wesley Publishing Company, 1964

[12] E.D. Rainville and P.E. Bedient, Elementary Differential Equations, Fifth Edition, Macmillan Publishing Co., Inc. (1974)

[13] J. Mathews and R.L. Walker, Mathematical Methods of Physics, Second Edition, W.A. Benjamin, Inc., pp. 235–236 (1970)

[14] W.H. Press, S.A. Teukolsky, W.T. Vetterling and B.P. Flannery, Numerical Recipes in Fortran, Second Edition, Cambridge University Press, pp. 818–880 (1994).

[15] A. Jeffrey, Handbook of Mathematical Formulas and Integrals, Third Edition, Elsevier Academic Press, pp. 426–431 (2004).

[16] E.R.G. Eckert and R.M. Drake, Jr., Analysis of Heat and Mass Transfer, McGraw-Hill, Inc., pp. 168–169 (1972).

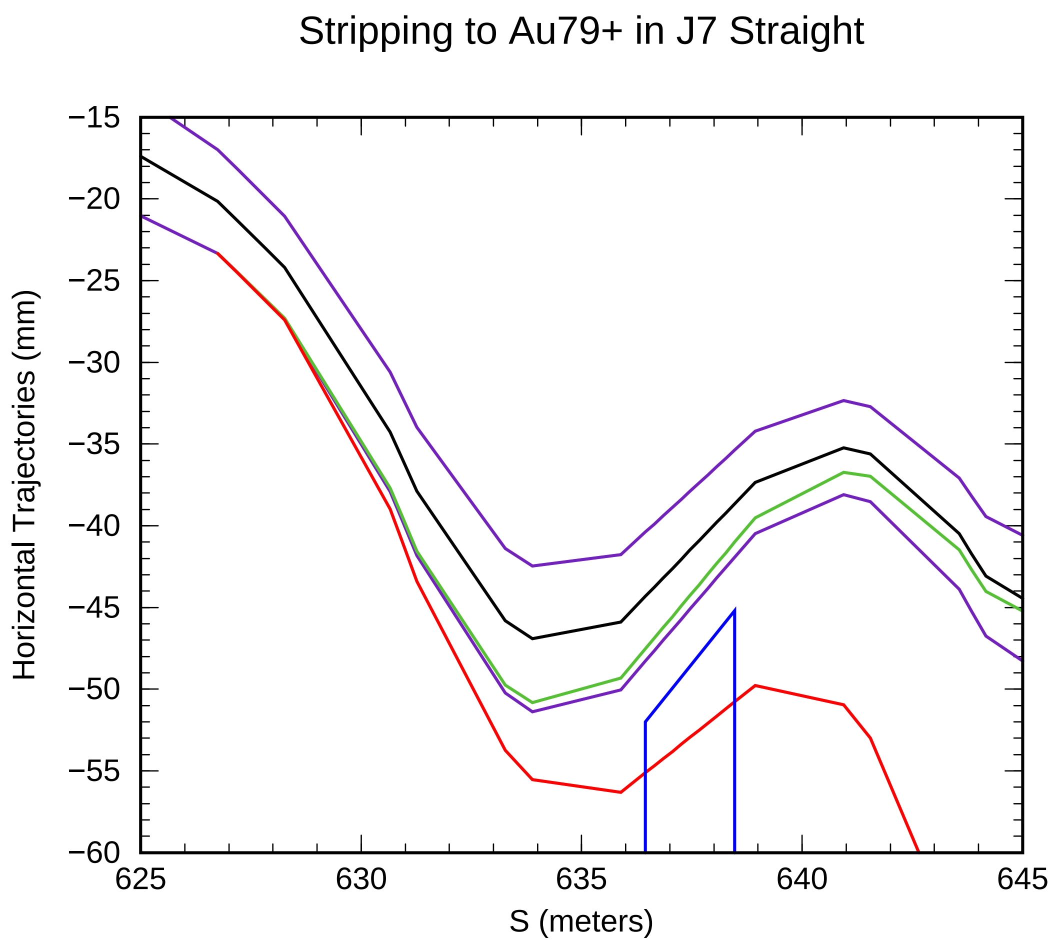

Figure 1: Here the red curve shows the trajectory of a gold ion that has been stripped to Au79+ by passing through a stripper located in the J7 straight. The green curve is the trajectory of an unstripped Au77+ ion with the same initial coordinates. The stripped ion is cleanly lost on the upstream face of the dump.

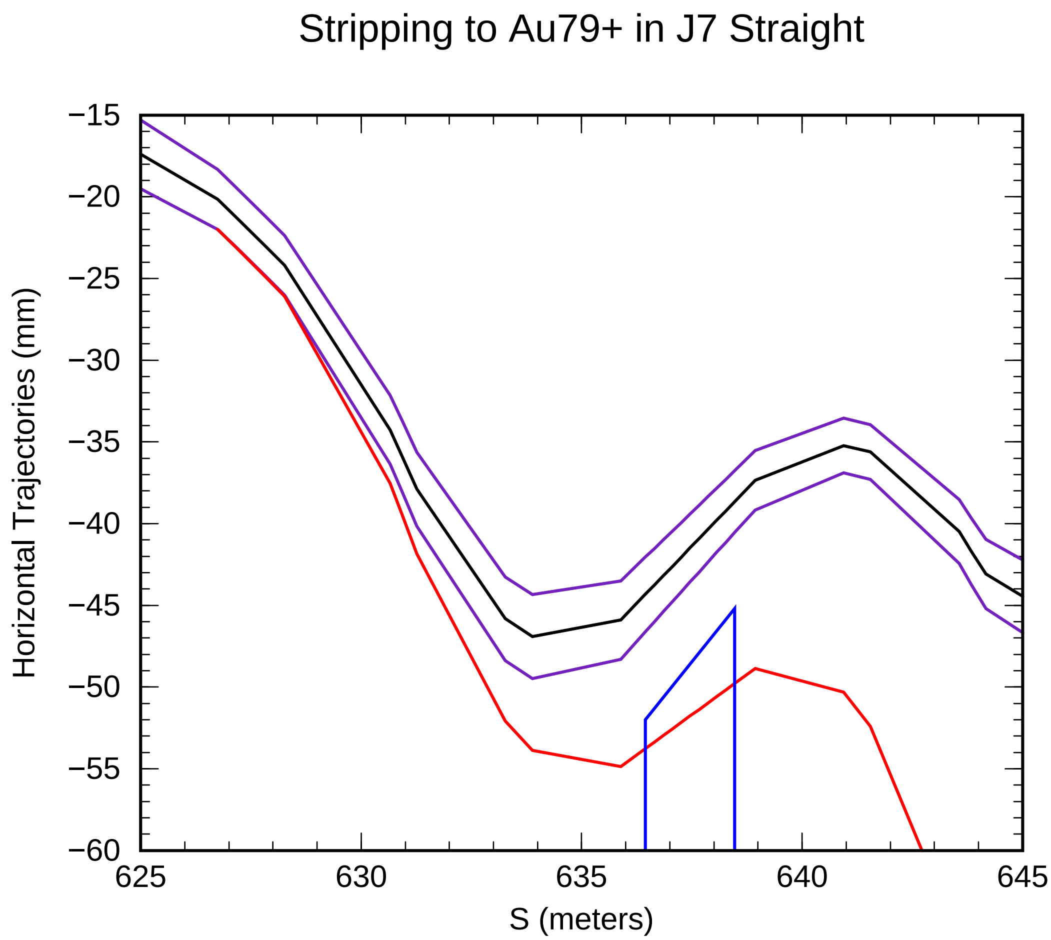

Figure 2: Holding the dump bump fixed we plung the J7 stripper further into the beam thereby reducing the circulating beam emittance while putting the stripped beam cleanly into the upstream face of the dump.

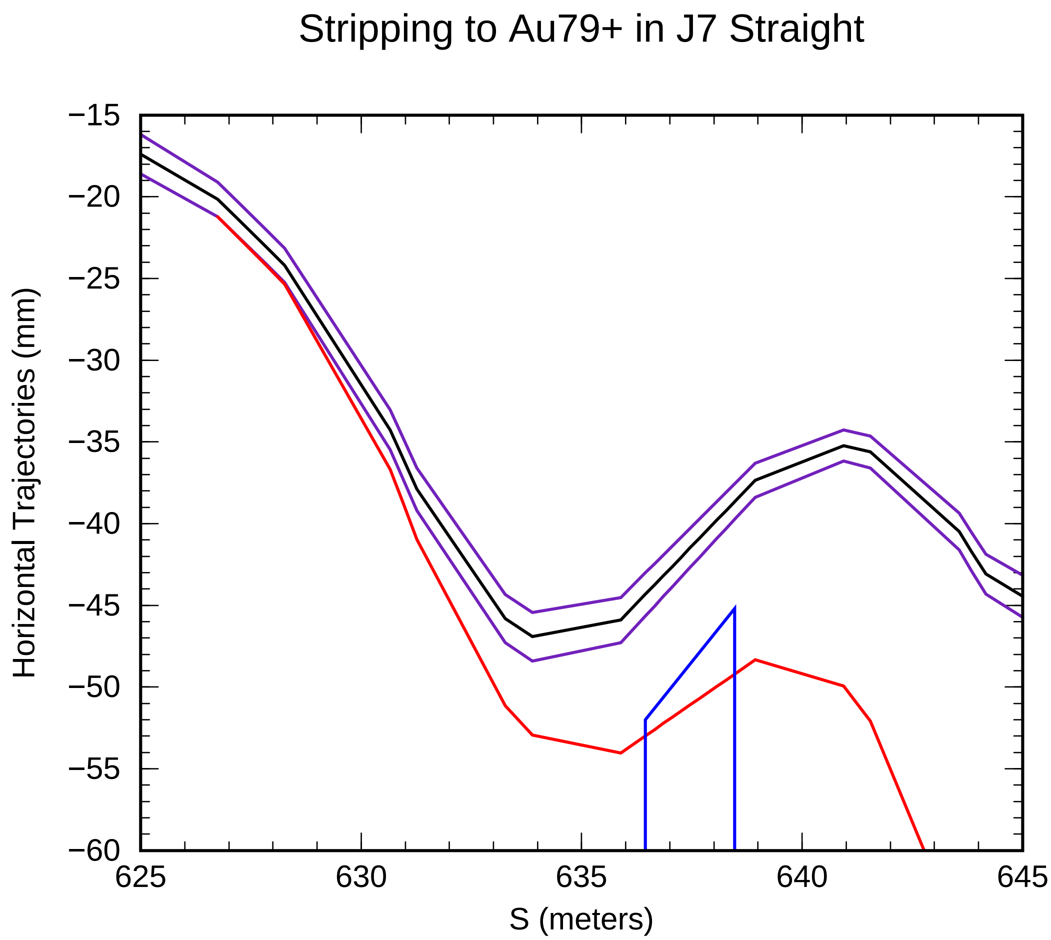

Figure 3: Holding the dump bump fixed we plung the J7 stripper further into the beam thereby reducing the circulating beam emittance while putting the stripped beam cleanly into the upstream face of the dump.

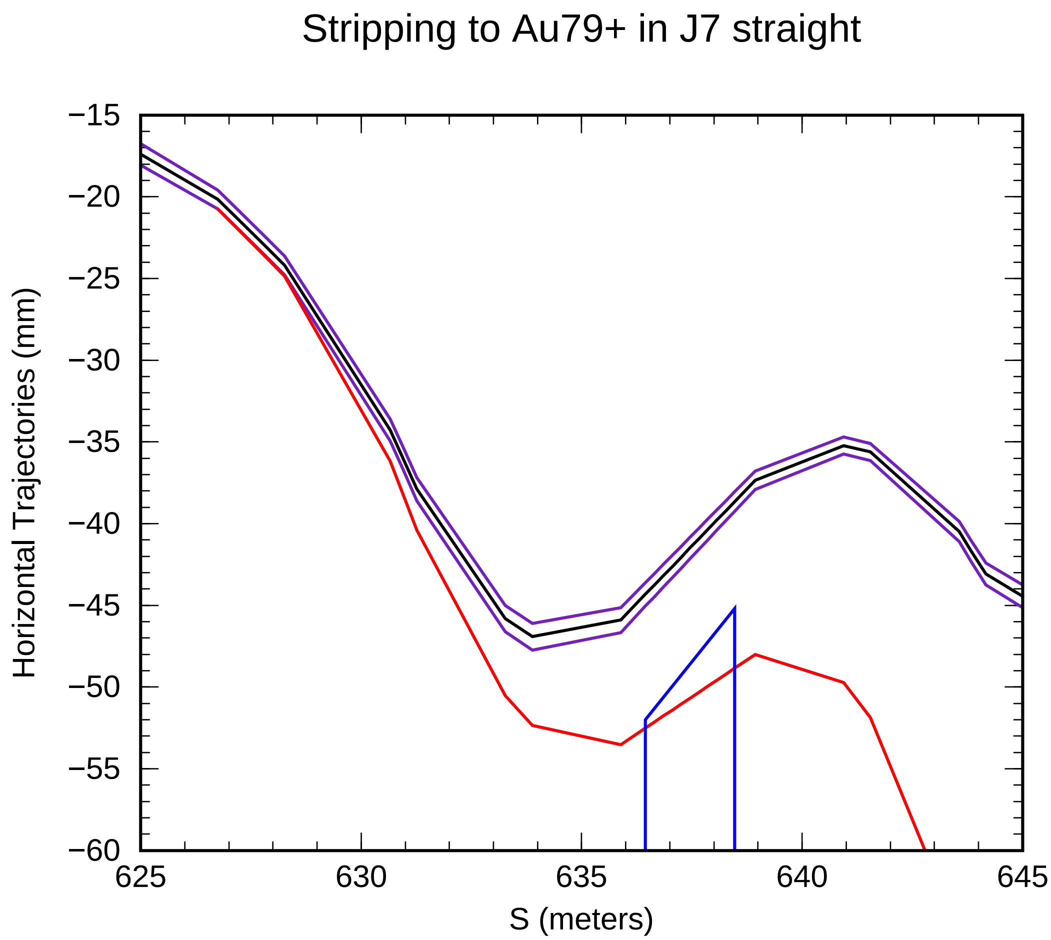

Figure 4: Holding the dump bump fixed we plung the J7 stripper further into the beam thereby reducing the circulating beam emittance while putting the stripped beam cleanly into the upstream face of the dump.

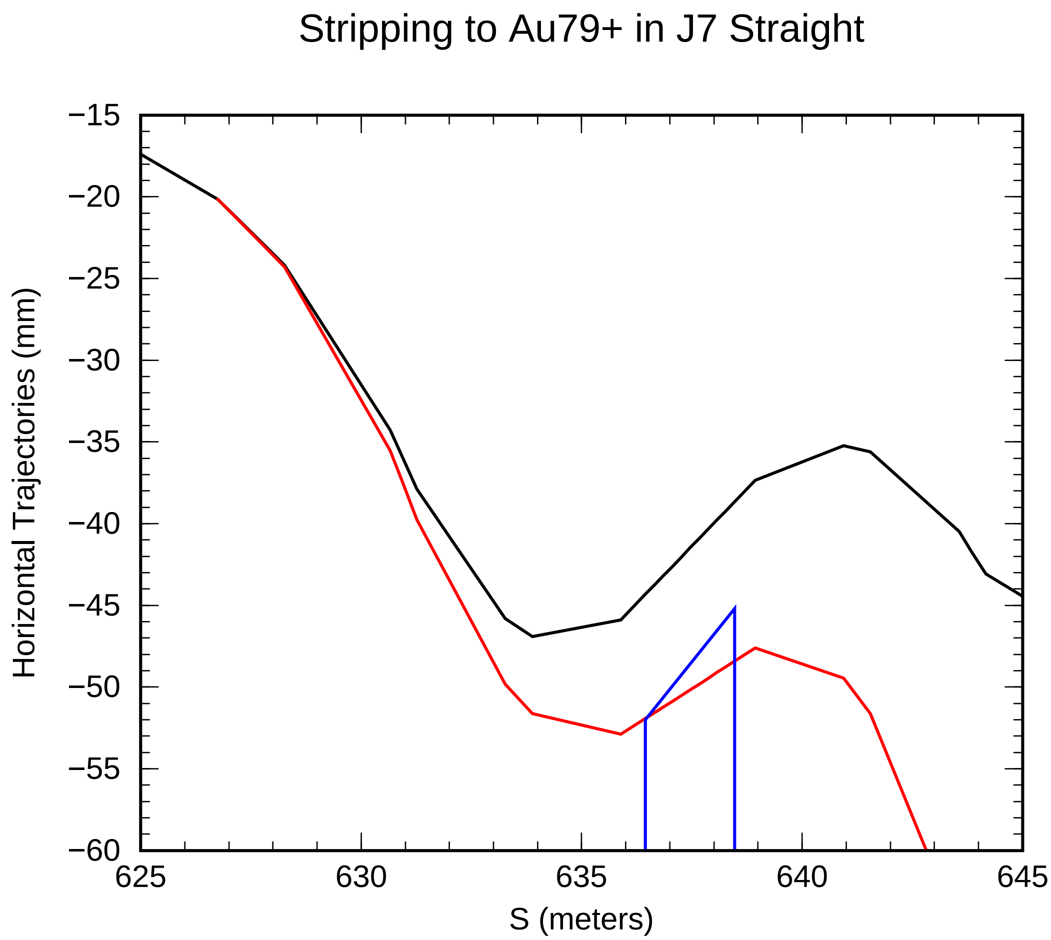

Figure 5: Holding the dump bump fixed we plung the J7 stripper further into the beam thereby reducing the circulating beam emittance while putting the stripped beam cleanly into the upstream face of the dump.

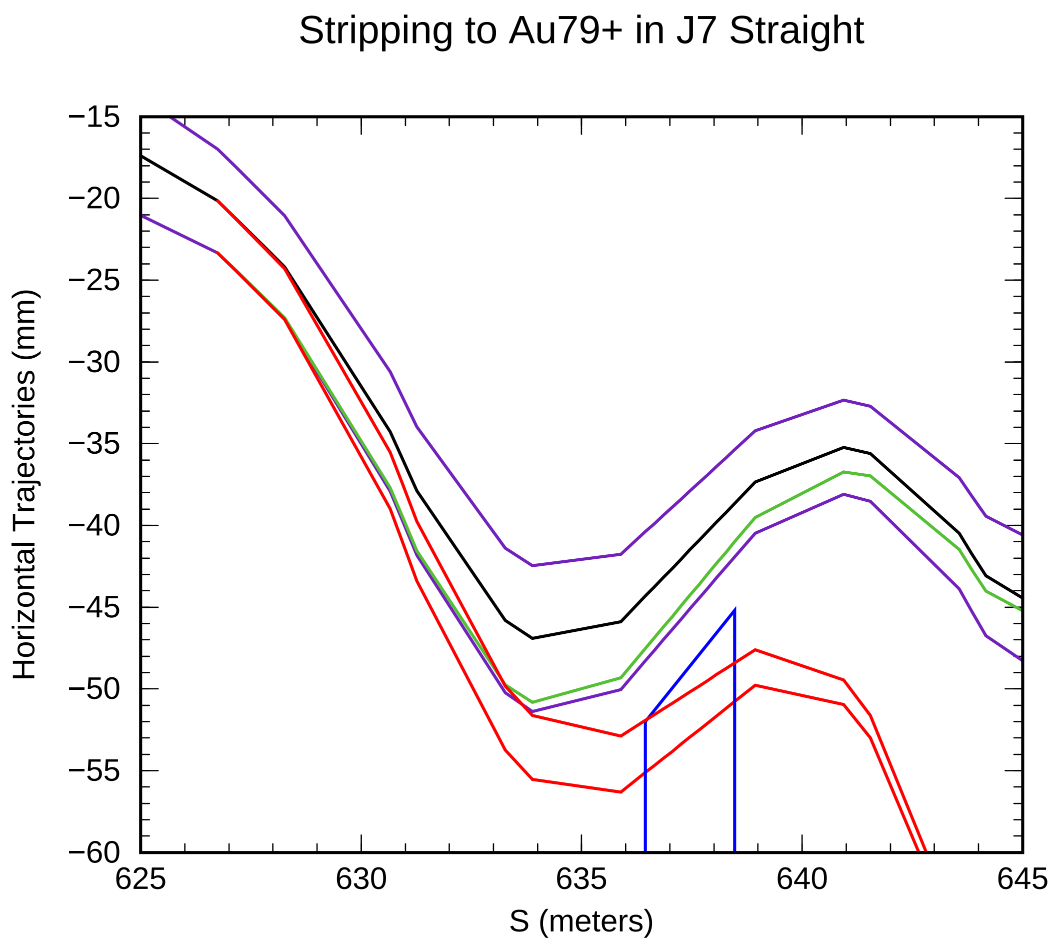

Figure 6: Here are the initial and final Au79+ ion trajectories obtained as the J7 stripper is plunged into the circulating beam. Note that the ions are lost at different locations on the face of the dump as the stripper moves into the beam. Note also that the magnet vacuum chamber aperture is at −3.406 inches (−86.5 mm).

Figure 7: Here is a current picture of the J7 straight. Most of the straight is occupied by the J7 sextupole. The J7 skew sextupole sits at the upstream end (to the left of the sextupole).

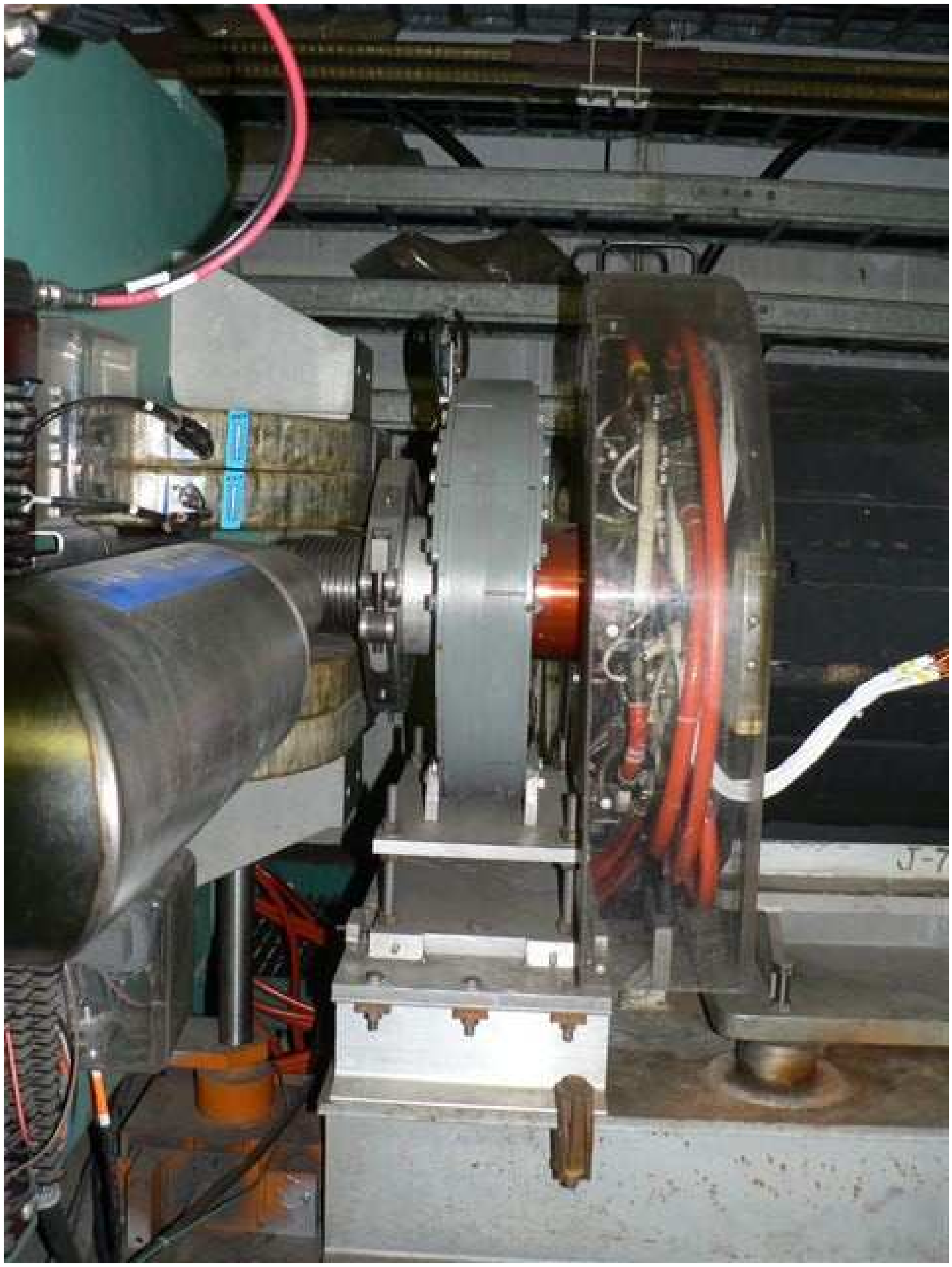

Figure 8: Here is a closer view of the skew sextupole at the upstream end of the J7 straight. This is what would have to be removed to make room for a stripper.

Figure 9: Here is a current picture of the F5 straight with the horizontal and vertical jump target mechanisms at the upstream (to the left) and downstream ends respectively.

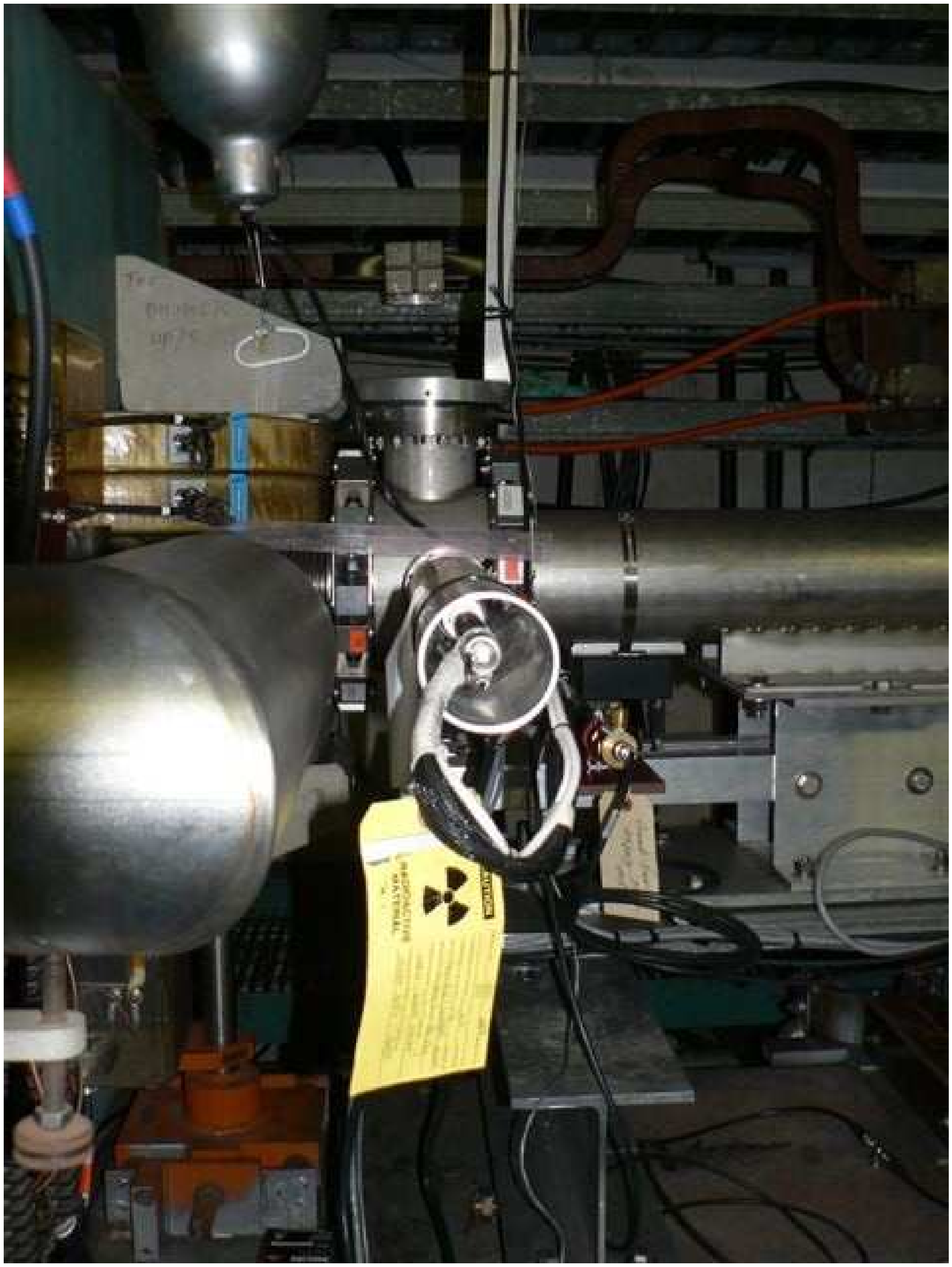

Figure 10: Here is a closer view of the horizontal jump target mechanism at the upstream end of the F5 straight. Our proposal is to move this mechanism to the J7 straight and use it to insert a stripper into the beam.

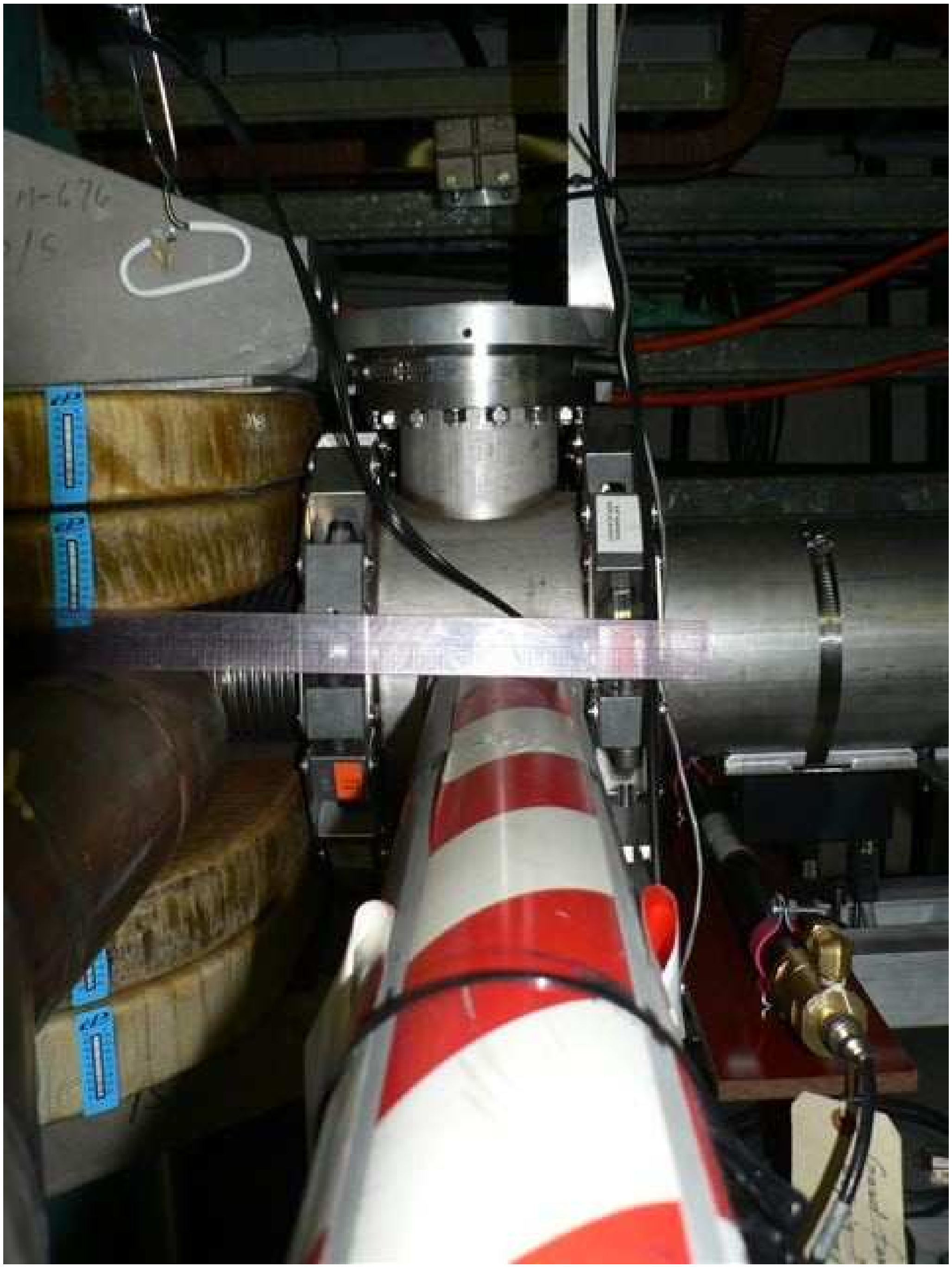

Figure 11: Here is an even closer view.

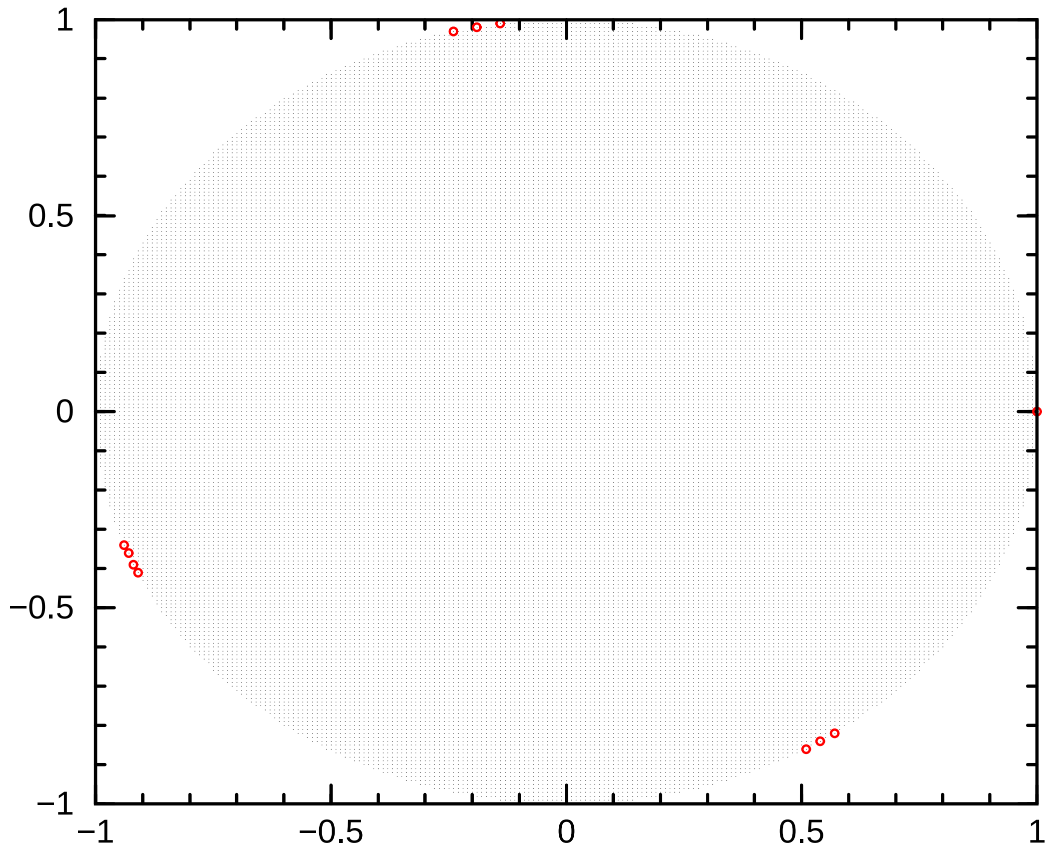

Figure 12: Initial beam distribution showing particles lost (red circles) on the jump target after 3 turns. The Target step per turn is 0.001 of the beam half-width. 1000 steps are required to remove all particles from the distribution. The horizontal tune is $Q = 0.281$.

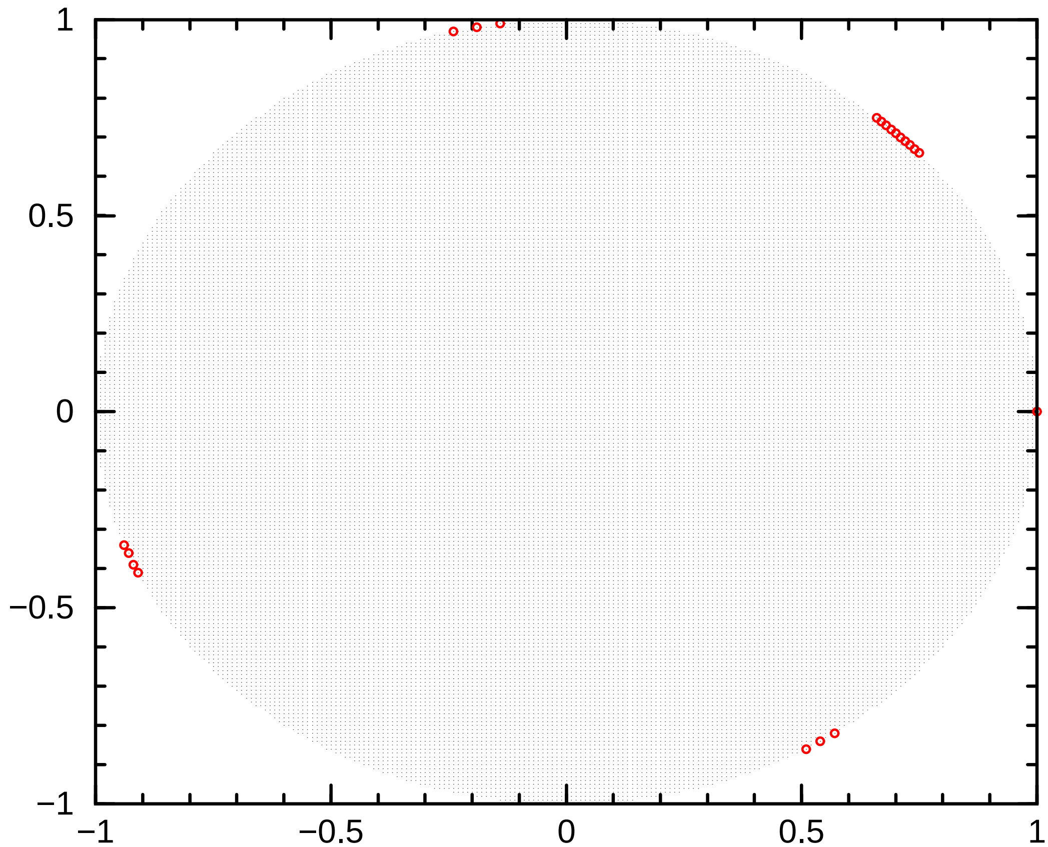

Figure 13: Initial beam distribution showing particles lost (red circles) on the jump target after 4 turns. The horizontal tune is $Q = 0.281$.

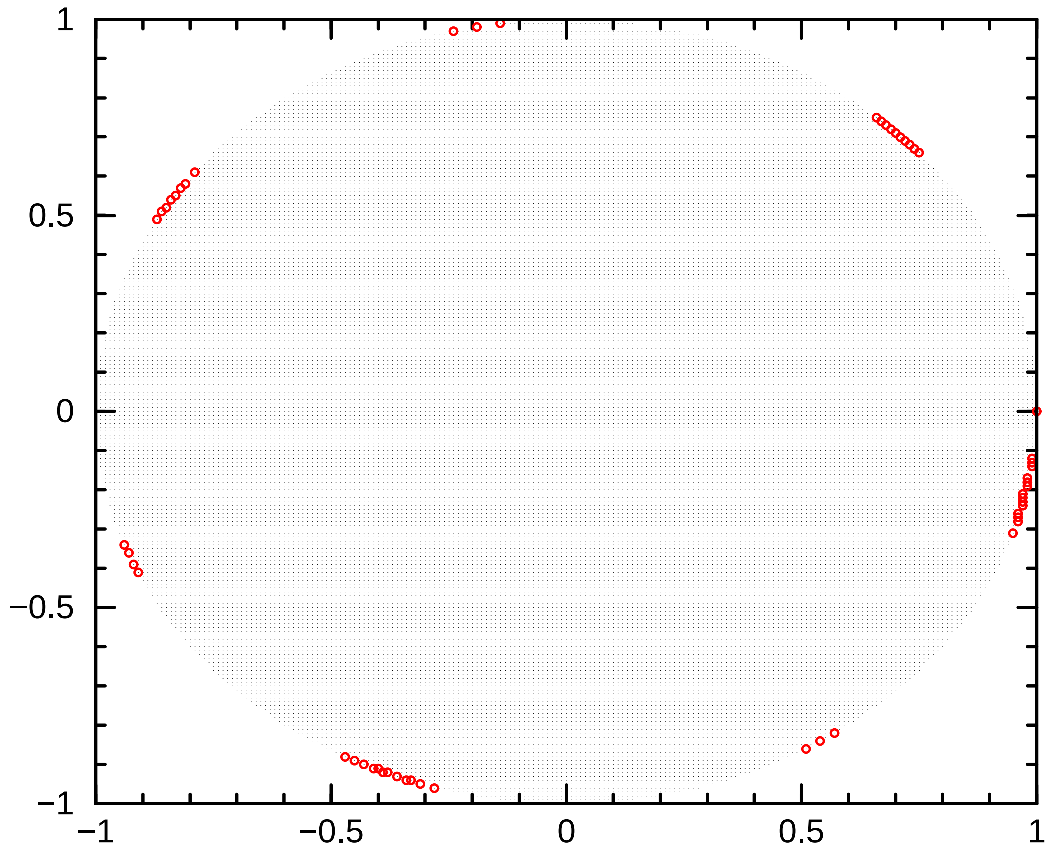

Figure 14: Initial beam distribution showing particles lost (red circles) on the jump target after 7 turns. The horizontal tune is $Q = 0.281$.

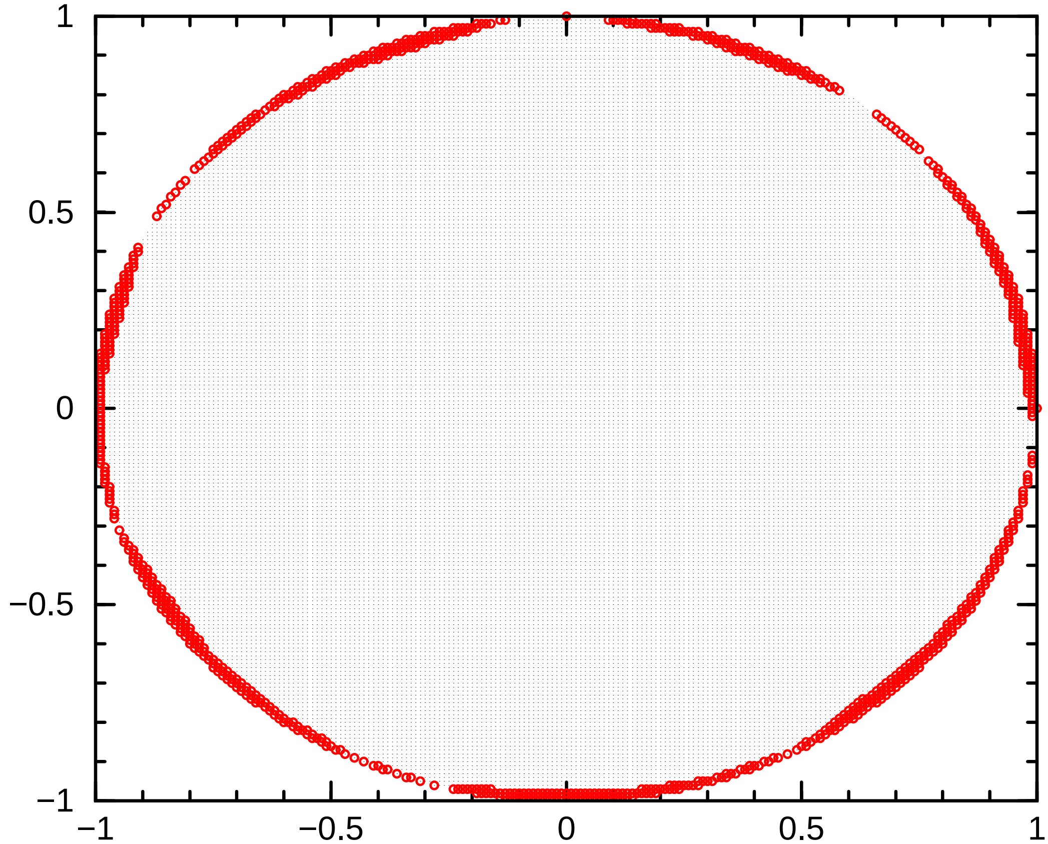

Figure 15: Initial beam distribution showing particles lost (red circles) on the jump target after 28 turns. The horizontal tune is $Q = 0.281$.

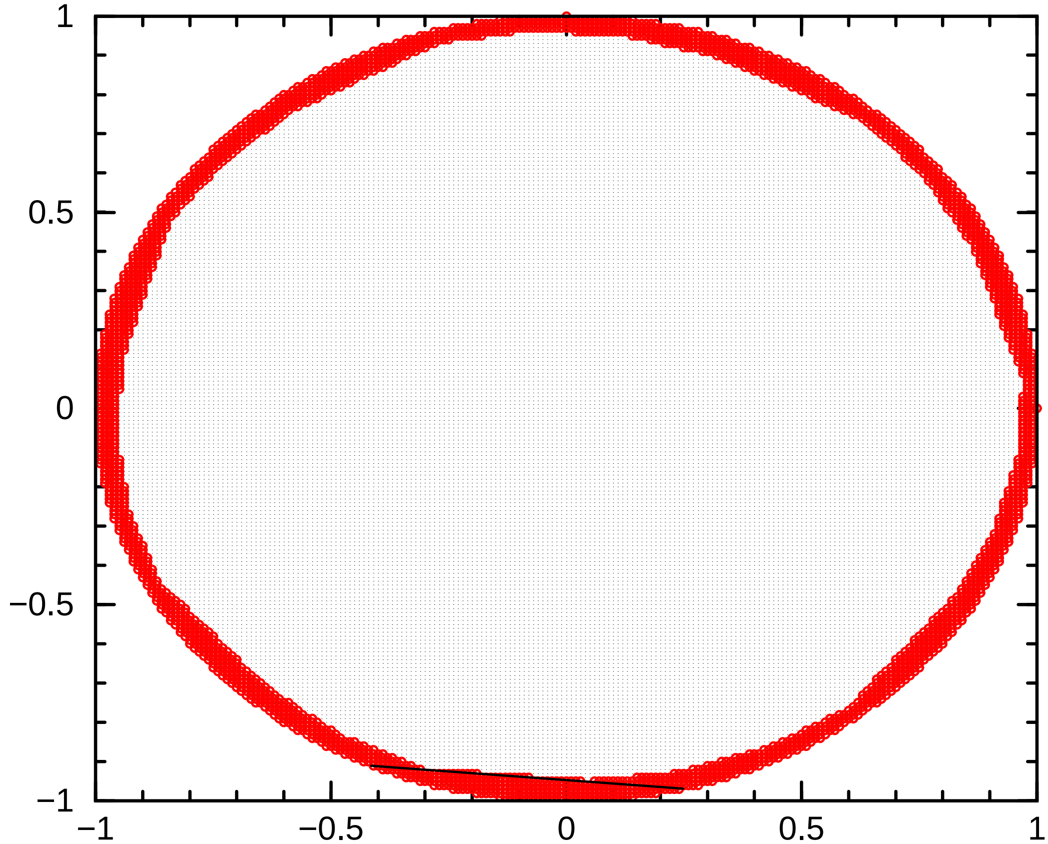

Figure 16: Initial beam distribution showing particles lost (red circles) on the jump target after 56 turns. The black line is the rotated image of the target edge after 56 turns. The horizontal tune is $Q = 0.281$.

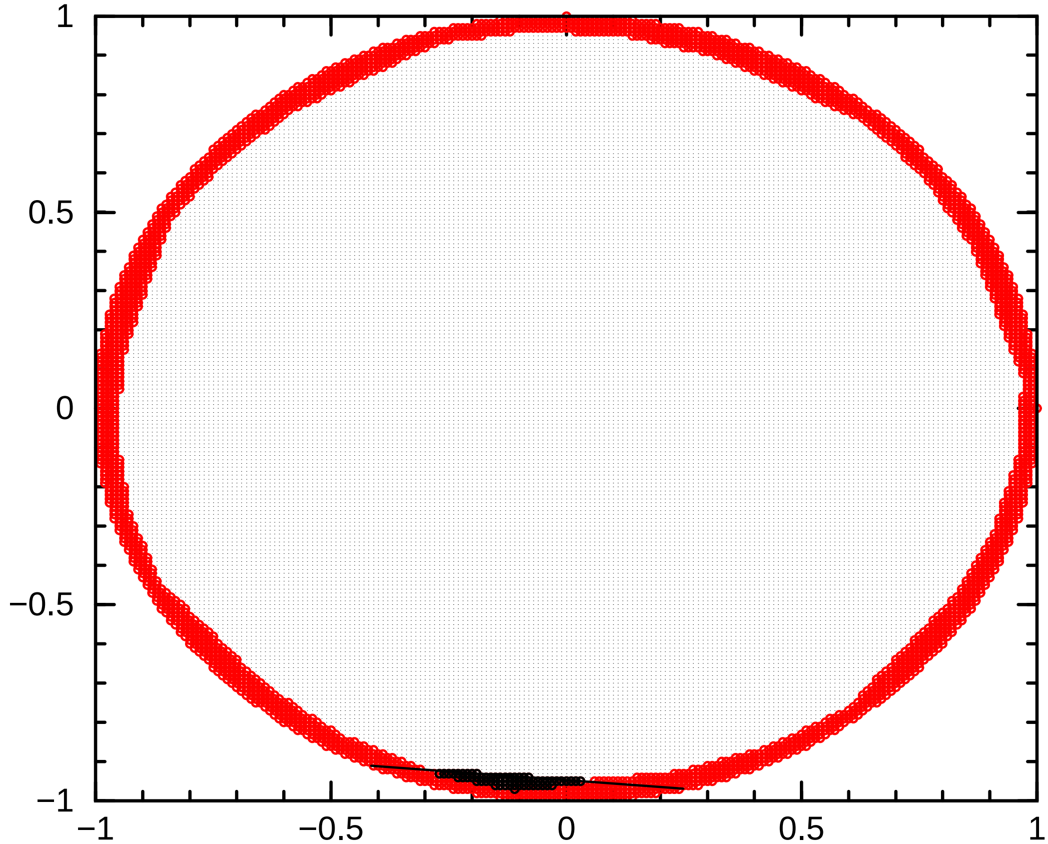

Figure 17: Initial beam distribution showing particles lost (red circles) on the jump target after 56 turns. The black line is the rotated image of the target edge after 56 turns. The black circles show the particles lost on the 56th turn. The horizontal tune is $Q = 0.281$.

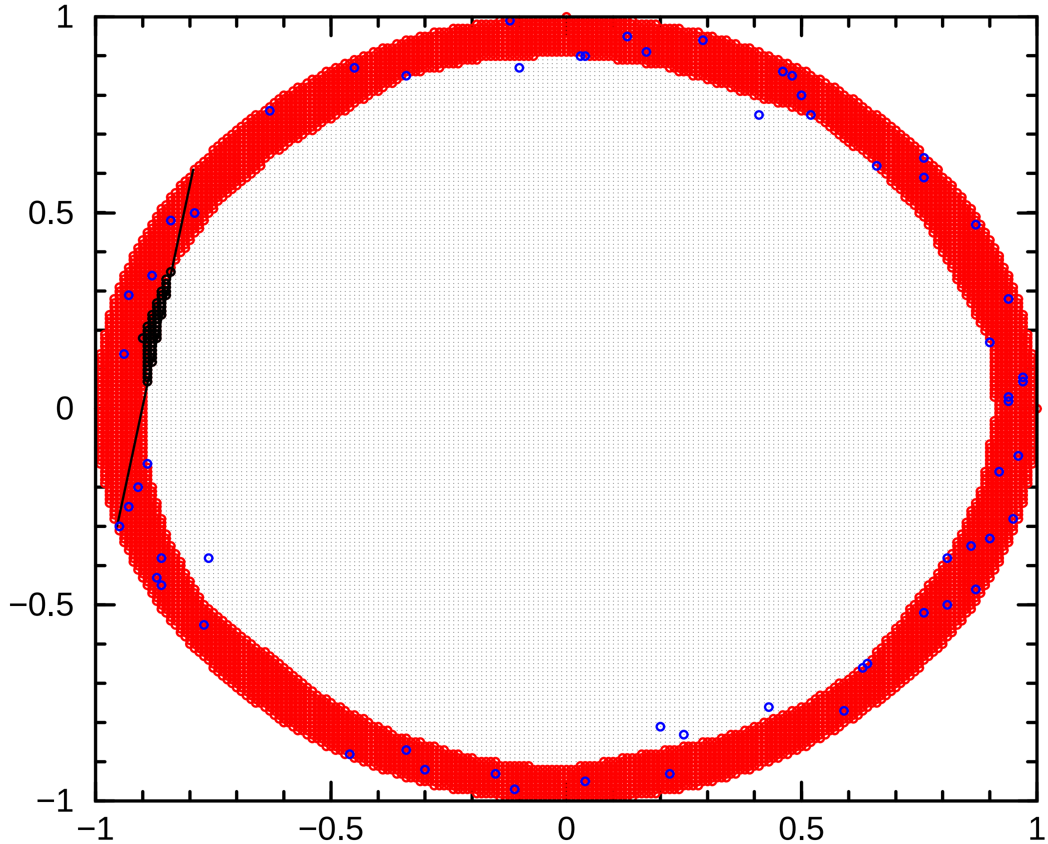

Figure 18: Initial beam distribution showing particles lost (red circles) on the jump target after 112 turns. The black line is the rotated image of the target edge after 112 turns. The black circles show the particles lost on the 112th turn. The blue circles show the particles lost the furthest from the target edge. The horizontal tune is $Q = 0.281$.

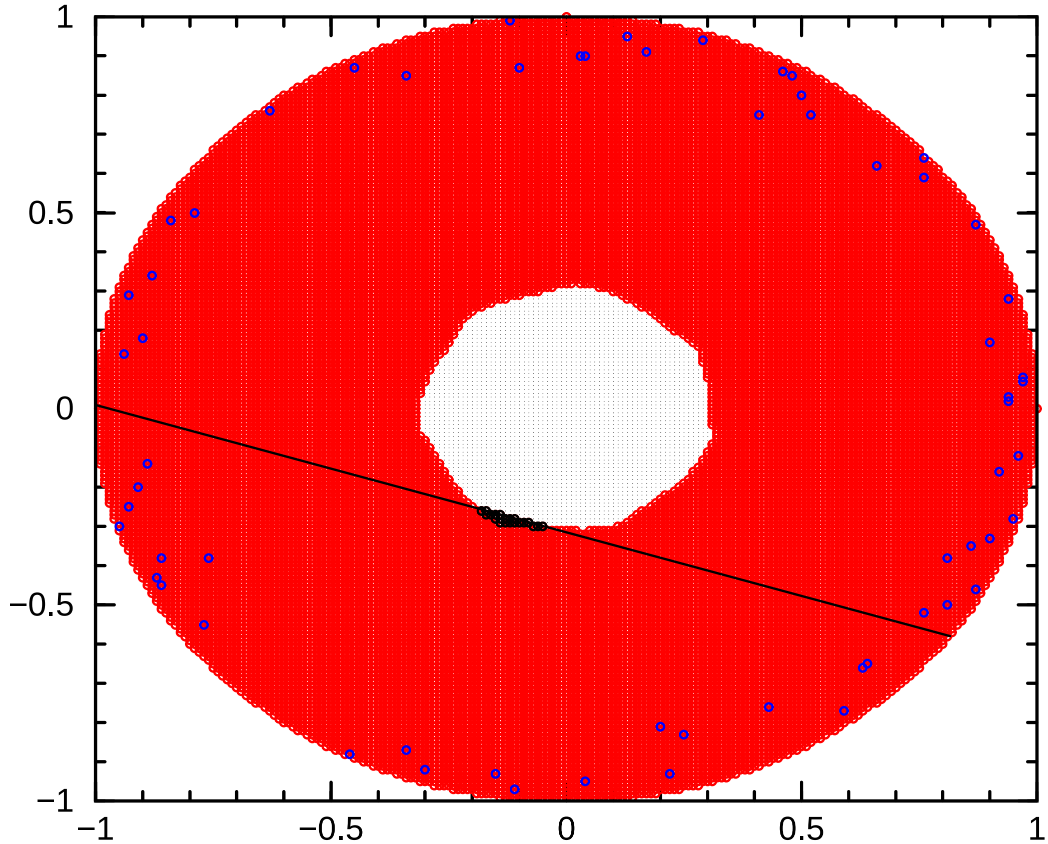

Figure 19: Initial beam distribution showing particles lost (red circles) on the jump target after 700 turns. The black line is the rotated image of the target edge after 700 turns. The black circles show the particles lost on the 700th turn. The blue circles show the particles lost the furthest from the target edge. The horizontal tune is $Q = 0.281$.

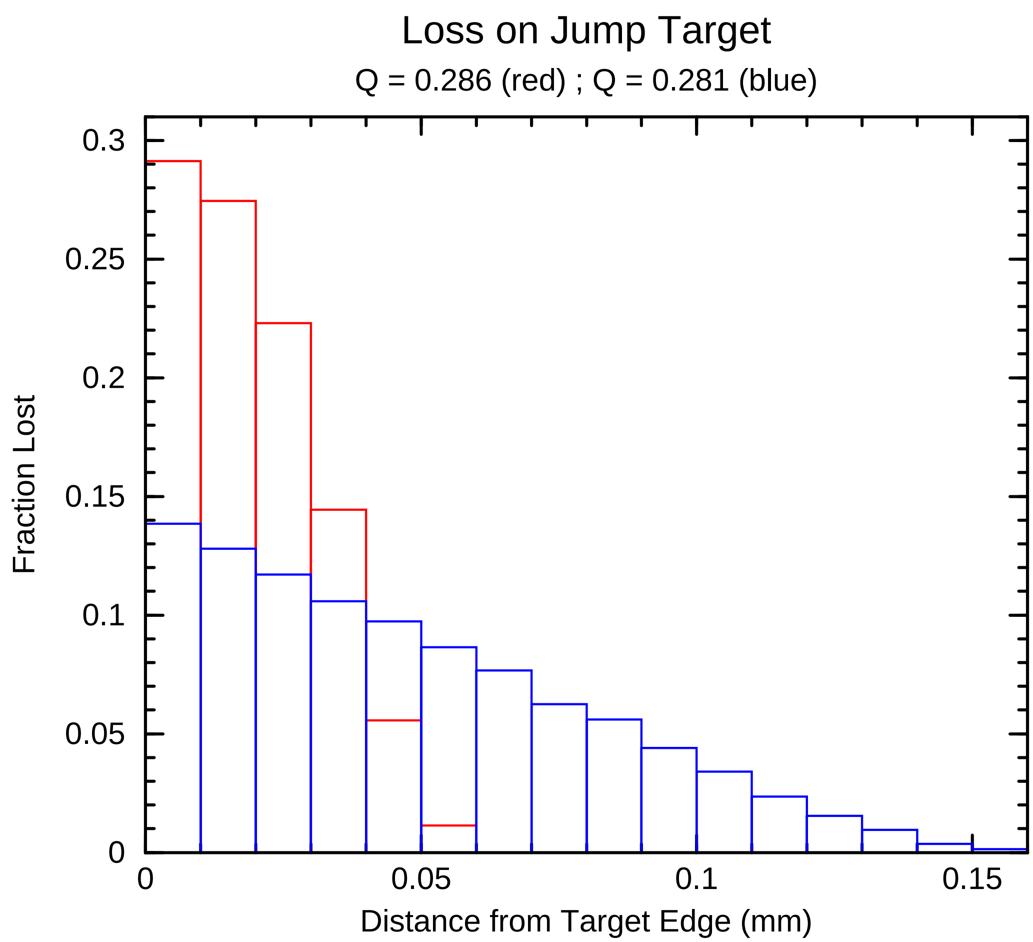

Figure 20: Loss on Jump Target. Target step per turn is 0.001 of beam half-width.

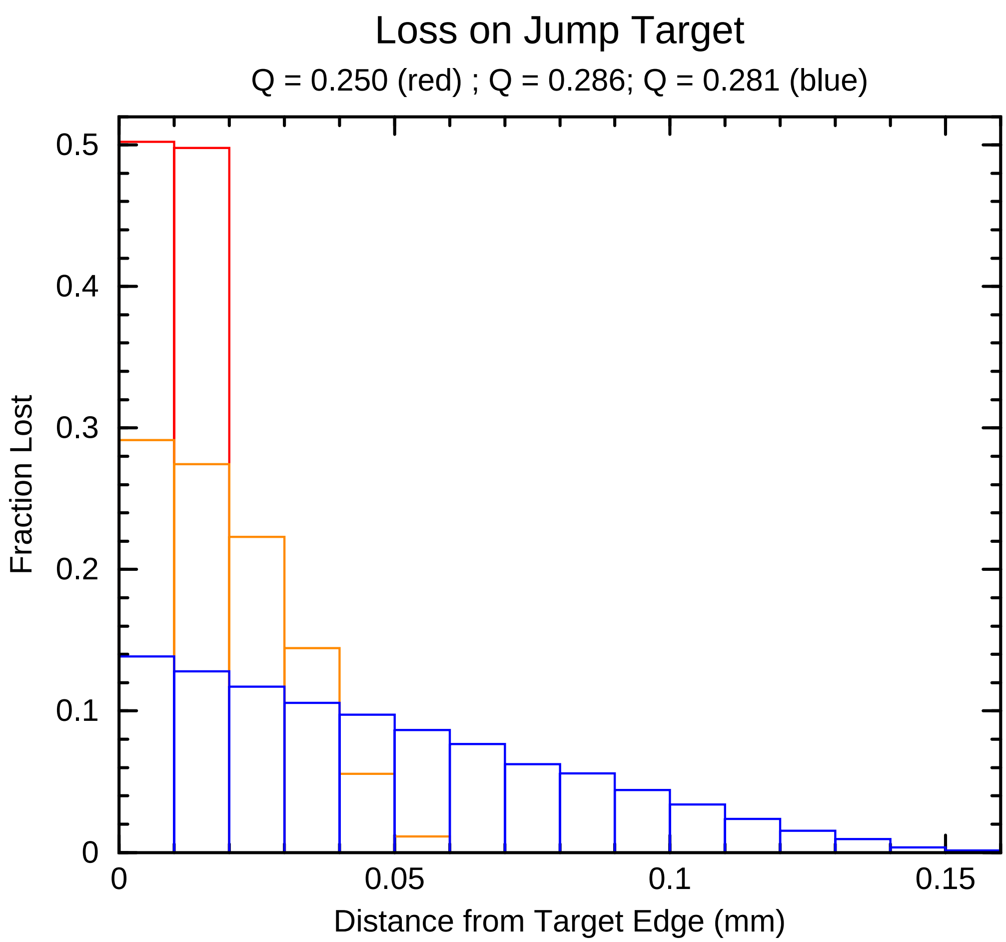

Figure 21: Loss on Jump Target. Target step per turn is 0.001 of beam half-width.

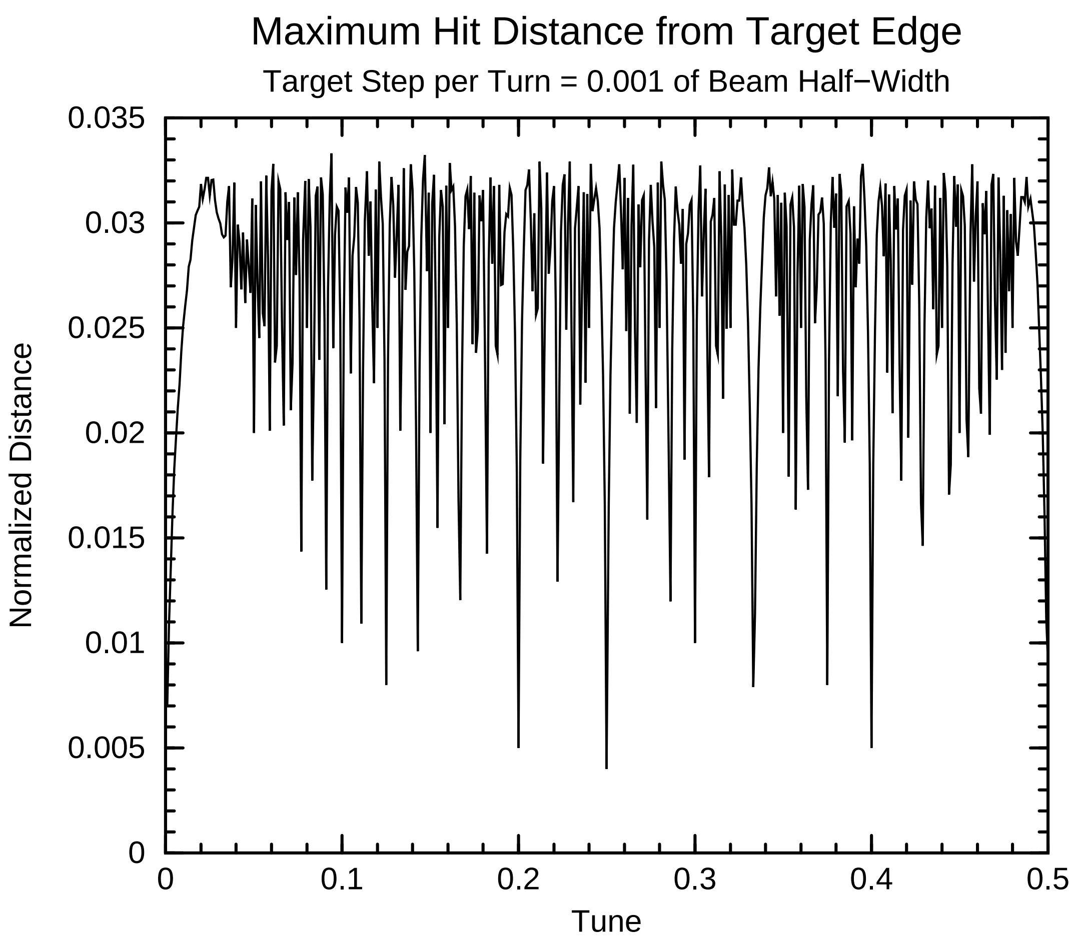

Figure 22: Hit X vs Q.

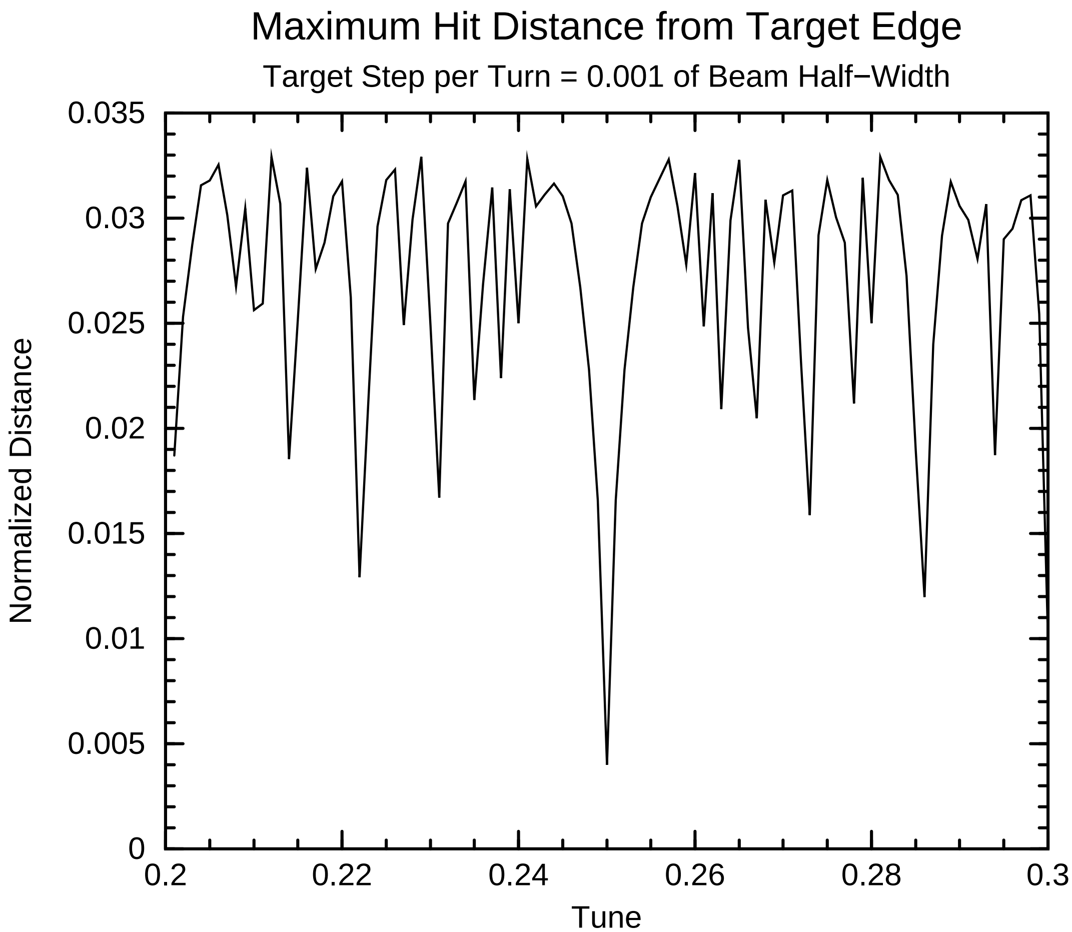

Figure 23: Hit X vs Q.

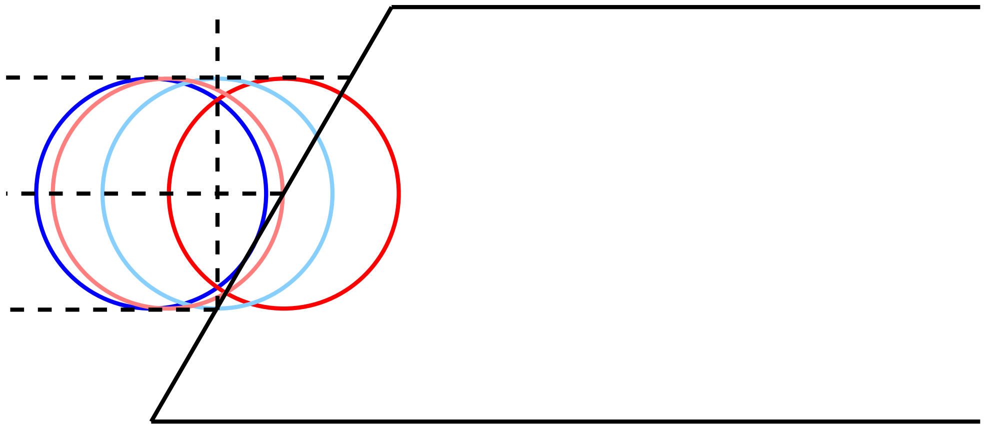

Figure 24: Jump Target Edge at $\theta = 60$ degrees. Width of projection of circle of radius R on edge is $W = 2R/\sin\theta$. Because of vertical motion, particles hit the lower half of the inclined edge first. As a result, the distance along the edge that is hit by beam is just $W/2$.

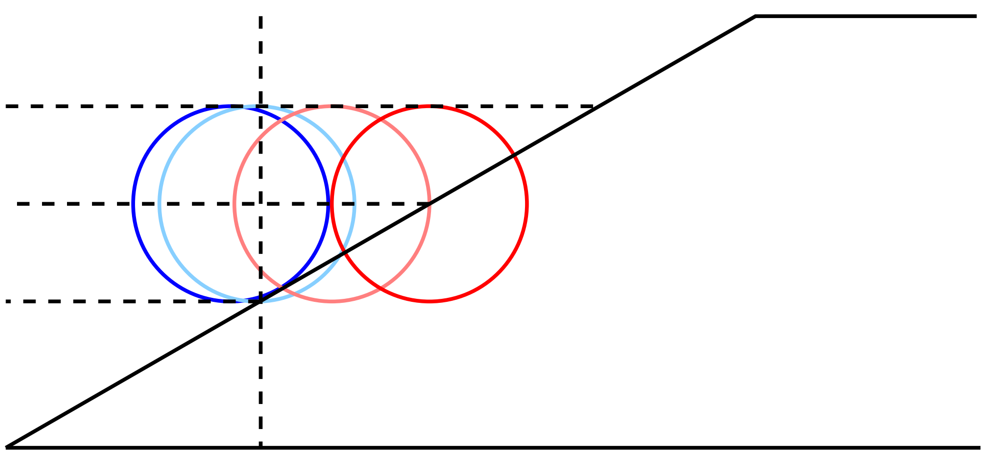

Figure 25: Jump Target Edge at 30 degrees.

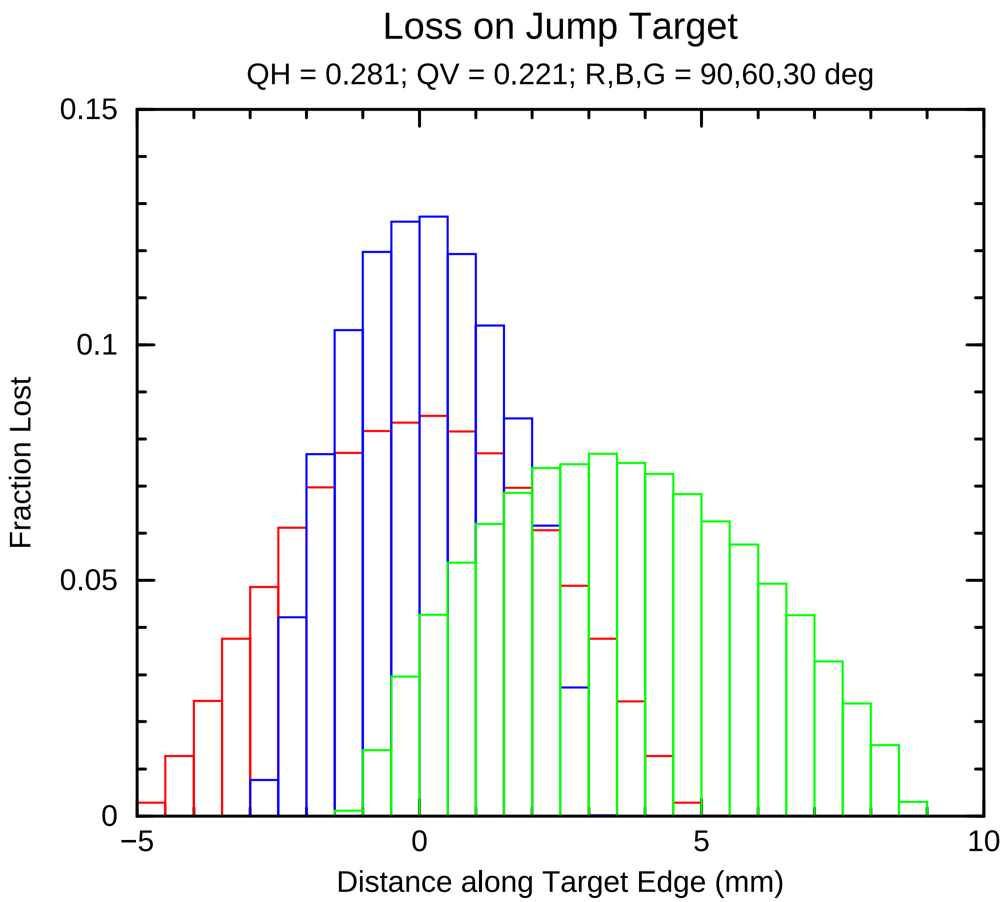

Figure 26: Loss along Target Edge. Red, Blue and Green histograms are for target edge at 90, 60 and 30 degrees respectively. (The angle for a vertical edge is 90 degrees.) Initial distribution is largest ball contained in a uniformly populated four-dimensional cube with 40^4 particles. We assume $\sqrt{\epsilon\beta} = 5$ mm in both planes. This is taken to be the smallest radius that contains all the particles. The target moves in horizontal steps of $0.001\sqrt{\epsilon\beta}$ per turn (2.7 μs) which gives a speed of 1.85 mm/ms. The times over which loss occurs on the target are 2.7, 3.12, and 5.4 ms for target edge at 90, 60, and 30 degrees respectively. During these times the target moves 5.0, 5.8 and 10 mm respectively in the horizontal direction. The horizontal and vertical tunes are $Q_H = 0.281$ and $Q_V = 0.221$.

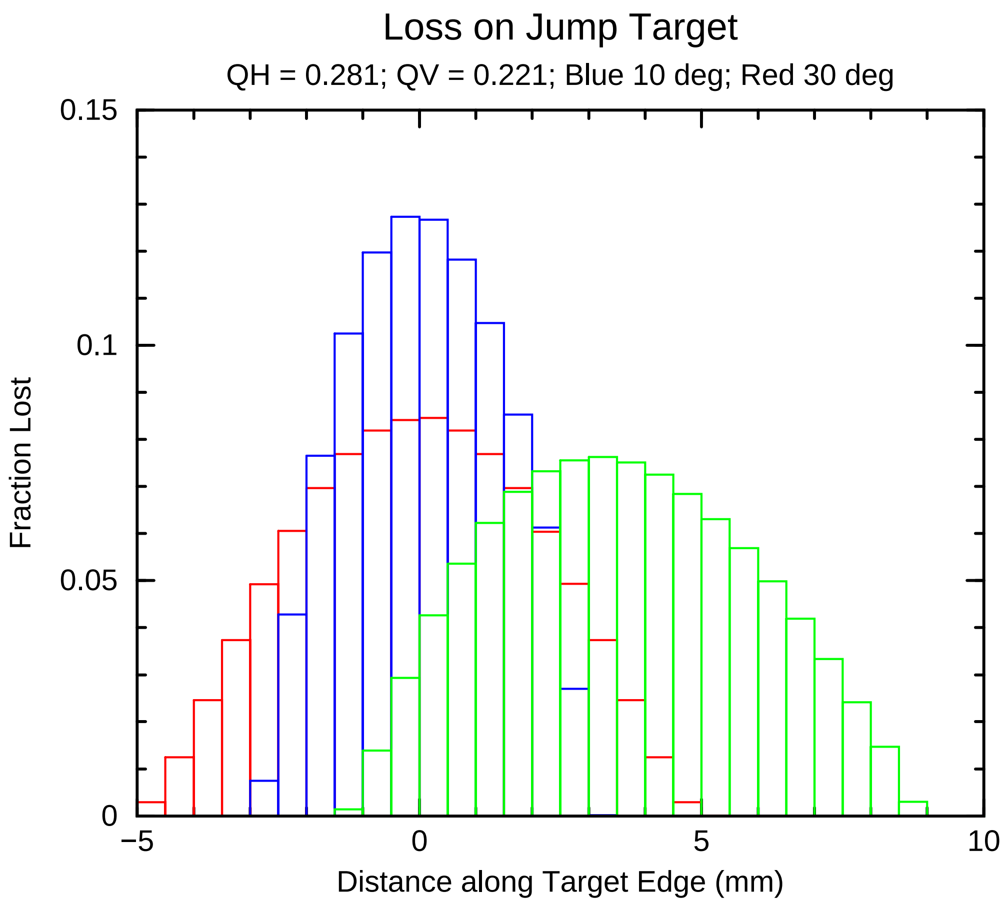

Figure 27: Loss along Target Edge. Red, Blue, Green = 90, 60, 30 degrees. Initial distribution is largest ball contained inside a uniformly populated four-dimensional cube now with 80^4 particles.

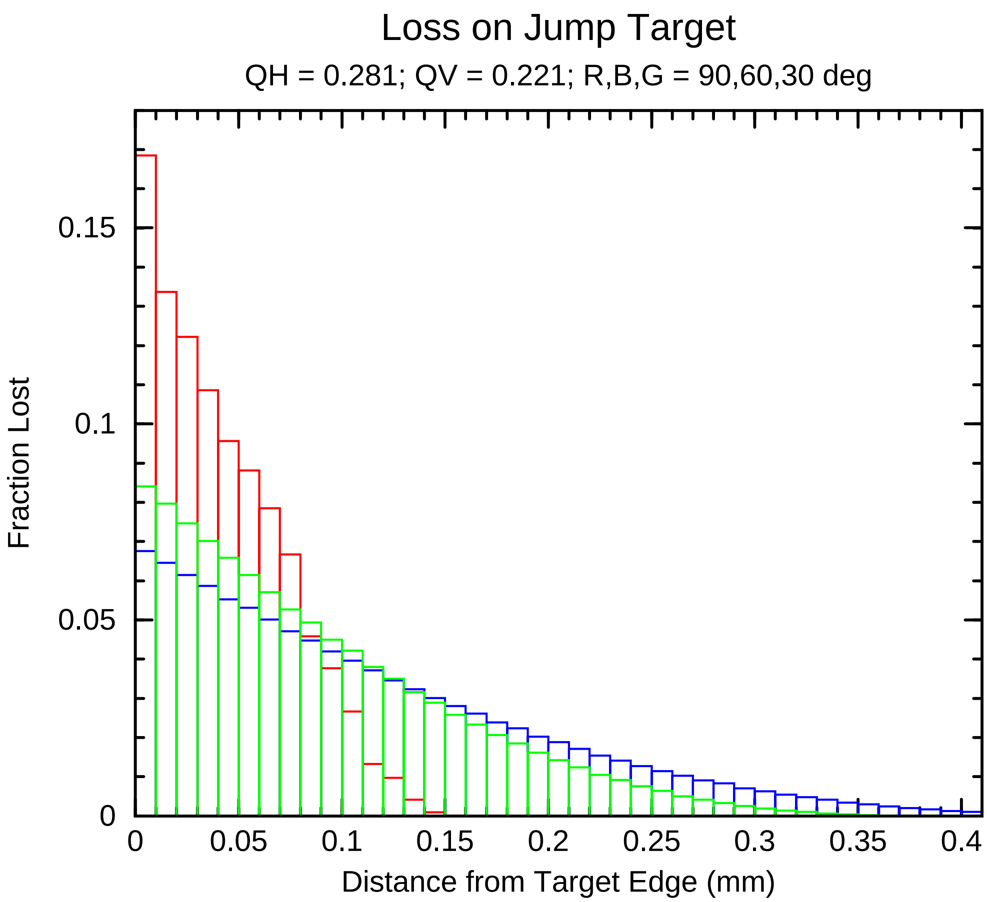

Figure 28: Loss on Target Edge. Red, Blue, Green = 90, 60, 30 degrees. Initial distribution is largest ball contained inside a uniformly populated four-dimensional cube with 40^4 particles.

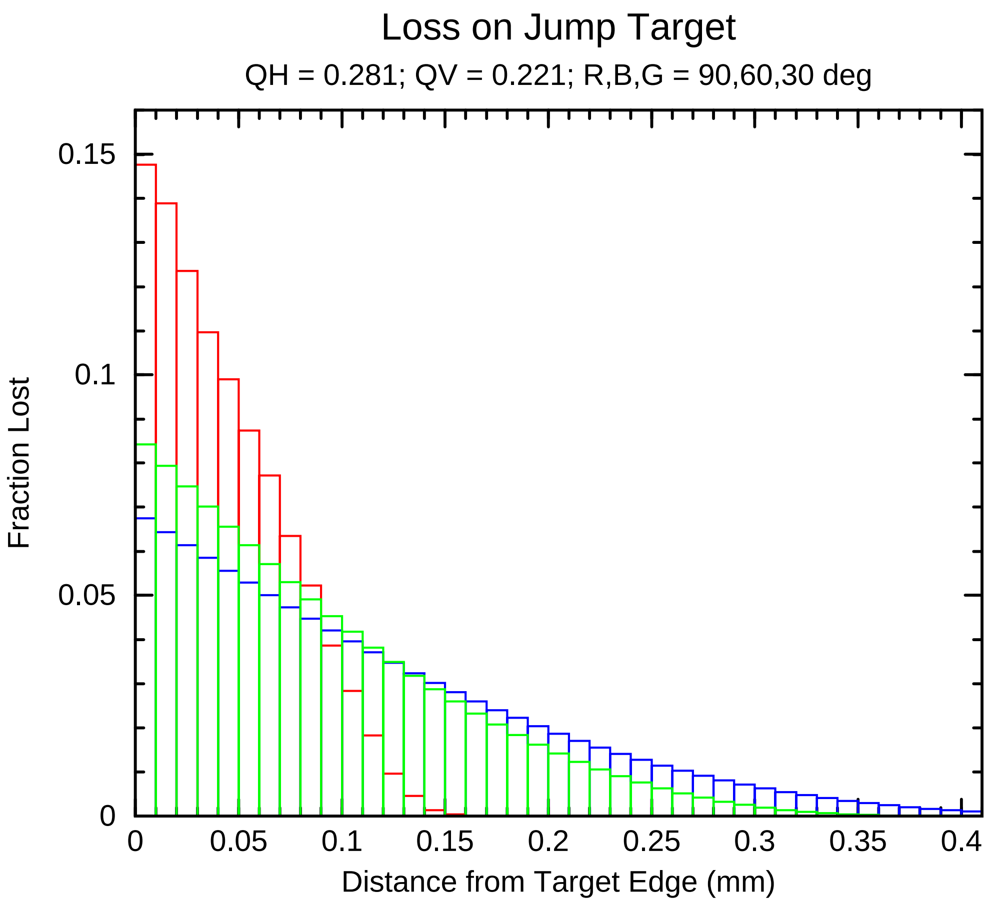

Figure 29: Loss on Target Edge. Red, Blue, Green = 90, 60, 30 degrees. Initial distribution is largest ball contained inside a uniformly populated four-dimensional cube now with 80^4 particles.

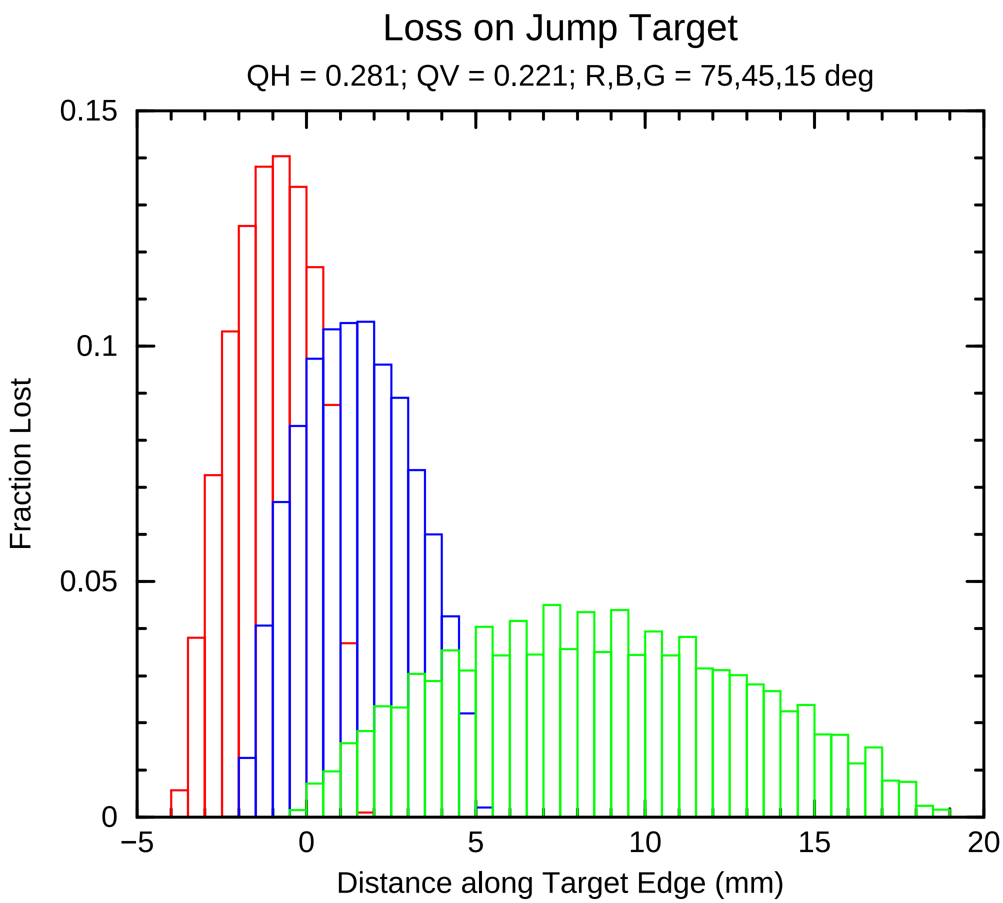

Figure 30: Loss along Target Edge. Red, Blue, Green = 75, 45, 15 degrees. Initial distribution is largest ball contained inside a uniformly populated four-dimensional cube with 40^4 particles.

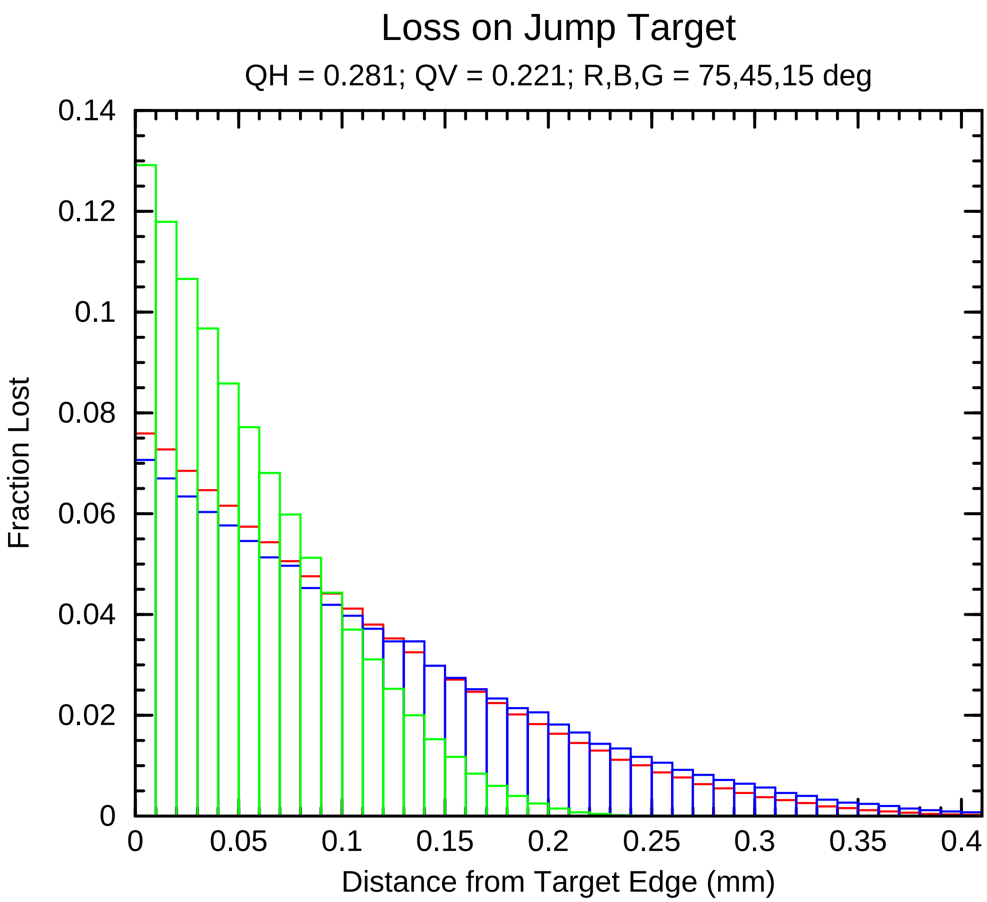

Figure 31: Loss on Target Edge. Red, Blue, Green = 75, 45, 15 degrees. Initial distribution is largest ball contained inside a uniformly populated four-dimensional cube with 40^4 particles.

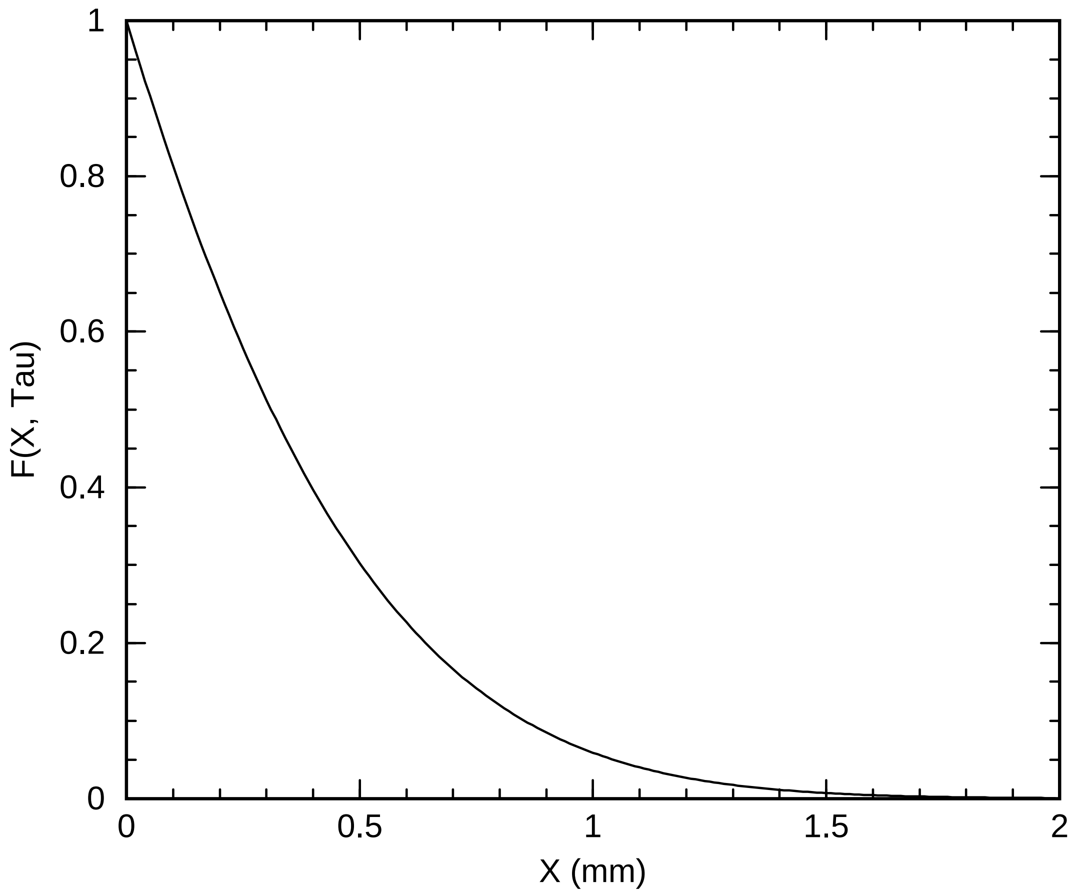

Figure 32: Plot of $F(x,\tau) = \exp\left(-\frac{x^2}{4\alpha\tau}\right) - \sqrt{\frac{\pi x^2}{4\alpha\tau}}\,\mathrm{erfc}\left(\frac{x}{\sqrt{4\alpha\tau}}\right)$. Here $\tau = 5$ ms and $\sqrt{4\alpha\tau} = 0.886$ mm.